AN ABSTRACT OF THE THESIS OF

Michael A. Shettles for the degree of Master of Science in Sustainable Forest Management presented on July 21, 2014.

Title: Error Propagation in Estimating Aboveground Biomass Using Terrestrial LiDAR.

Abstract approved:

Temesgen Hailemariam

Broad-scale estimates of above ground forest biomass (AGB) are typically produced by applying individual-tree equations to inventory data consisting of measurements from probabilistically or purposively selected trees. The associated uncertainty for these estimates depends primarily on three sources of error that interact and propagate: (1) measurement error, the quality of the tree-level measurement data used as inputs for the individual-tree equations; (2) model error, the uncertainty about the equations predictions themselves; and (3) sampling error, the uncertainty due to having obtained a probabilistic or purposive sample, rather than a census, of the trees on a given area of forest land. Often only sampling error is accounted for, resulting in an underestimation of the actual uncertainty for estimates of AGB. With an increased importance placed on accurate estimation of AGB for broader scales comes an increased need to credible portray the true magnitude of their associated uncertainties.

One additional benefit of accounting for all three sources of uncertainty is that it provides an opportunity to observe possible gains in precision to be had by addressing measurement error. Terrestrial LiDAR is a high-precision instrument that has proven useful in forest inventory applications. Several studies have assessed the performance of this technology in extracting tree-level metrics. However, no research efforts exist that have taken this information and subsequently assessed the impact of this measurement performance on the total uncertainty of broad-scale estimates of forest-related parameters, such as AGB.

This study aims to compare the total propagated error for two sets of regional-level component equations for lodgepole pine AGB, and for two sets of high-precision instruments by accounting for all three of these sources of error. The two sets of models compared included a set of newly-developed component ratio method (CRM) equations, and a set of component AGB equations currently used by the Forest Inventory and Analysis (FIA) unit of the United States Department of Agriculture (USDA) Forest Service. Instrument comparisons made were between a phase-based terrestrial laser scanner (TLS) and traditional forest inventory instruments, which in this study were a Spencer combination tape and a Trupulse Laser Rangefinder 360R. Monte Carlo simulations were used to propagate measurement, model and sampling error, and to compare total uncertainty between models, and between instruments. Input variables for the equations were diameter at breast height, total tree height and height to crown base; these were extracted from the terrestrial LiDAR data through the creation of automated algorithms.

Relative contributions for measurement, model and sampling error using the current regional equations were 5%, 2% and 93%, respectively, and 13%, 55% and 32%, respectively using the CRM equations. Relative standard error (RSE) values for the current regional and CRM equations with all three error types accounted for were 20.7% and 36.8%, respectively. Relative contributions for measurement, model and sampling error for the TLS were 5%, 70% and 25%, respectively, and 11%, 66% and 23%, respectively using the traditional instruments. RSE values for the TLS and traditional instruments, with all three error types accounted for, were 52.1% and 54.4%, respectively. Results for the model comparisons indicate that per acre estimates of AGB using the CRM equations are far less precise than those produced with the current set of regional equations. Results for the instrument comparisons indicate the TLS can in fact reduce uncertainty in broad-scale estimates of AGB attributed to measurement error.

Error Propagation in Estimating Aboveground Biomass Using Terrestrial LiDAR

by

Michael A. Shettles

A THESIS

submitted to

Oregon State University

in partial fulfillment of

the requirements for the

degree of

Master of Science

Presented July 21, 2014

Commencement June 2015

Master of Science thesis of Michael A. Shettles presented on July 21, 2014.

APPROVED:

Major Professor, representing Sustainable Forest Management

Head of the Department of Forest Engineering, Resources and Management

---

Dean of the Graduate School

I understand that my thesis will become part of the permanent collection of Oregon State University libraries. My signature below authorizes release of my thesis to any reader upon request.

Michael A. Shettles, Author

ACKOWLEDGEMENTS

To say that I am grateful for the contributions, guidance, support and opportunities given by my major professor, Temesgen Hailemariam, would be a bit of an understatement. From my days as an undergraduate in Forest Management here at the OSU College of Forestry, to this final point, no person at this institution am I more indebted to for continually fostering my professional development than him. Extended thanks are due as well for the appreciated contributions of my committee members Andrew Gray, Professor Thomas Hilker and Professor Lisa Ganio during the conception, analysis and writing portions of my thesis work. My parents also deserve mentioning for their offerings of encouragement throughout all of my educational pursuits, tactfully questioning my logic at the most appropriate of moments.

It is also my pleasure to offer profound thanks for those who, not only have facilitated my completion of my graduate work in a timely and successful manner, but have (arguably more importantly) also helped mitigate the intermittent slippage of sanity associated with extended stays down in the dungeon-like office known as Peavy 053-A. Thanks to Richard Gabriel for quality training on using the FARO scanner and for answering all of my random questions. Your work with the scanner the year prior to me deciding to use it planted the seed of interest. Thanks to Elijah Allensworth for helping whack back the brush and for carrying the heavy wooden signs while I had the honor of lugging around the $40,000 scanner over slash and entanglements of tree roots. Thanks to Krishna Poudel and Joonghoon Shin for all the statistical advice, and for the valued camaraderie, especially during my hectic first term while we were a trio of TA's. Thanks to Lacey Jeroue for being an excellent classmate during the eight

classes we took together and for simply putting up with me in general down in our office. I am awfully talkative when I drink too much coffee. You offered more inadvertent life lessons as a result of our time around each other than you will ever know! Thanks to Dr. Bianca Eskelson for kindly offering several moments of insight relating to my project, and for offering preparatory materials for the FOR 525-Forest Modeling class months in advance. Finally, profound thanks to the field and lab summer crew of 2013 that I worked alongside during the data collection effort.

CONTRIBUTION OF AUTHORS

Dr. Temesgen Hailemariam, Dr. Lisa Ganio, Dr. Andy Gray and Dr. Thomas Hilker provided valued critique and contributions to the writing of Chapters 2 and 3.

TABLE OF CONTENTS

Page

Chapter 1: GENERAL INTRODUCTION 1

Chapter 2: COMPARISON OF UNCERTAINTY IN PER UNIT AREA ESTIMATES OF ABOVEGROUND BIOMASS FOR TWO SELECT MODEL SETS 5

Introduction 5

Component Ratio Method 8

Methods 11

Study Locations 11

Field Data 11

Models Compared 13

Measurement Error Variability 16

Integrating Simulated Measurement Errors into Model Uncertainty 17

Integrating Model Errors into Sampling Uncertainty 19

Results and Discussion 23

Model Predictions and Uncertainty 23

Per Unit Area Estimates and Uncertainty 25

Conclusion 28

TABLE OF CONTENTS (Continued)

Page

References....30

CHAPTER 3: ADDRESSING UNCERTAINTY IN PER UNIT AREA ESTIMATES OF ABOVEGROUND BIOMASS USING TERRESTRIAL LIDAR....37

Introduction....37

Terrestrial LiDAR....38

Methods....41

TLS Field Scanning Procedure....41

TLS Point Cloud Registration and Processing....42

Tree Parameter Extraction from Selected Scan Data....43

Digital Terrain Model....43

Tree Detection....44

Uphill Side of the Tree and Total Height....45

Diameter at Breast Height....46

Height to Crown Base....47

Error Propagation....49

TABLE OF CONTENTS (Continued)

Page

Results and Discussion 49

Measurement Errors 49

Model Predictions and Uncertainty 53

Per Unit Area Estimates and Uncertainty 54

Conclusion 55

References 57

CHAPTER 4: GENERAL CONCLUSION 67

BIBLIOGRAPHY 71

APPENDIX 75

LIST OF FIGURES

Figure Page

Figure 3.1: Planar view of scan points depicting typical field scanning setup with four checkerboard targets setup around the sample tree, located middle right 63

Figure 3.2: Filtered overhead 3D view of registered point cloud. Black circles denote scan locations around the sample tree, located right center.....63

Figure 3.3: Clipped sample tree from surrounding forest depicted in Figure 2.2.....64

Figure 3.4: Birds eye view of detection slice taken at 1.37m above the lowest point in the point cloud. Unrestricted subset included branches and foliage located within the height range of the slice 64

Figure 3.5: Birds eye view of detection slice taken at 1.37m above the lowest point in the point cloud. Unrestricted subset included branches and foliage located within the height range of the slice 65

Figure 3.6: Graph of point frequency versus elevation, depicting the 0.1m height bins. Actual total tree height is 16.95m 65

Figure 3.7: Fourth-order Polynomial Fit to the Frequency Height Profile. The first inflection point from the ground was theorized to correspond to the location of HTCB 66

Figure 3.8: Graph of intensity values versus elevation for 0.1m height bins. Subjectively determined subset threshold is shown in red 66

LIST OF TABLES

Table Page

Table 2.1: Summary statistics of the measurements errors for HT and HTCB 33

Table 2.2: Model predictions and RMSE values for CRM ratios, CRM tree-level estimates and tree-level estimates for the regional equations, without measurement error. Total minus foliage, the sum of the tree-level component estimates, is used as another means for comparison between the models. Tree-levels units are in kilograms of dry biomass. HTCB 33

Table 2.3: Model predictions and RMSE values for CRM ratios, CRM tree-level estimates and tree-level estimates for the regional equations, with measurement error. Total minus foliage, the sum of the tree-level component estimates, is used as another means for comparison between the models. Tree-levels units are in kilograms of dry biomass. 34

Table 2.4: Model RRMSE values for CRM ratios, CRM tree-level estimates and tree-level estimates for the regional equations, with and without measurement error. Total minus foliage, the sum of the tree-level component estimates, is used as another means for comparison between the models. 34

Table 2.5: Per hectare estimates and SE values for CRM and regional equations, without accounting for measurement or model error. Total minus foliage, the sum of the per acre component estimates, is used as another means for comparison between the models. Tree-levels units are in kilograms of dry biomass per hectare.....35

Table 2.6: Per hectare estimates and SE values for CRM and regional equations, accounting for model error. Total minus foliage, the sum of the per acre component estimates, is used as another means for comparison between the models. Tree-levels units are in kilograms of dry biomass per hectare 35

Table 2.7: Per hectare estimates and SE values for CRM and regional equations, accounting for both measurement and model error. Total minus foliage, the sum of the per acre component estimates, is used as another means for comparison between the models. Tree-levels units are in kilograms of dry biomass per hectare. 36

Table 2.8: RSE values for CRM and regional equations, for all three scenarios depicted in the previous three tables. Total minus foliage, the sum of the per acre component estimates, is used as another means for comparison between the models……...36

Table 3.1: TLS technical data 59

LIST OF TABLES (Continued)

Table Page

Table 3.2: Summary statistics of the measurements errors for STM and TLS.....59

Table 3.3: Model predictions and RMSE values for CRM ratios and CRM tree-level estimates without measurement error. Tree-levels units are in kilograms of dry biomass 60

Table 3.4: Model predictions for CRM ratios and CRM tree-level estimates with measurement error, for STM and TLS. Tree-levels units are in kilograms of dry biomass 60

Table 3.5: Model RMSE values for CRM ratios and CRM tree-level estimates with measurement error, for STM and TLS. Tree-levels units are in kilograms of dry biomass 61

Table 3.6: Per hectare estimates and SE values for CRM equations, without accounting for measurement or model error. Units are in kilograms of dry biomass per hectare ..61

Table 3.7: Per hectare estimates and SE values for CRM equations accounting for model error. Units are in dry kilograms of biomass per hectare.....62

Table 3.8: Per hectare estimates and SE values for CRM equations accounting for model error. Units are in dry kilograms of biomass per hectare.....62

Table 3.9: RSE values for CRM equations accounting for model and measurement error.....62

Chapter 1: General Introduction

As concerns grow over the effects associated with rises in atmospheric carbon, the objective of producing reliable stock and change estimates for forest carbon stores becomes increasingly important (Heath et al. 2008). While estimates of forest carbon at various scales are becoming important variables sought after by forest managers, direct measurement of carbon stored in forest vegetation is difficult to quantify, particularly at broader scales. Therefore, relationships between the dry weight of forest vegetation, commonly referred to as forest biomass, and its carbon content are often used to obtain estimates of forest carbon. Estimates of forest biomass are usually obtained first, with these estimates subsequently then being converted to estimates of carbon using empirically-derived species-specific conversion factors. Biomass as a unit of measure has also proven useful for purposes of quantifying forest bioenergy resources for use in alternative energy markets.

Forest biomass stores that are quantified and reported almost exclusively include the above-ground portion due to the complex and exceeding difficult manner of sampling and measurement required for estimating the below-ground portion (Lu 2006). Furthermore, different methods exist for estimating biomass for overstory trees and for understory shrubs and forbs. Examined here are the species-specific equations used for predicting above ground biomass (AGB) of individual trees. These equations result from linear and non-linear regressions of observed values of biomass on easily measurable tree-level attributes, such as diameter at breast height and total tree height. Observed values are primarily gathered during destructive sampling efforts that aim to

ascertain total biomass for all major tree components, such as bark, branches, foliage and bole wood.

Forest managers routinely apply these individual-tree equations to inventory data consisting of measurements from probabilistically or purposively selected trees to obtain broad-scale estimates of AGB. These broad-scale estimates are often reported with accompanying reliability statements, describing the magnitude of certainty behind these estimates of AGB. The reliability of these estimates produced using this approach depends on three primary sources of uncertainty, or error, that interact and propagate: (1) the quality of the tree-level measurement data used as inputs for the individual-tree equations; (2) the uncertainty about the equations predictions themselves; and (3) the uncertainty due to having obtained a probabilistic sample, rather than a census, of the trees on a given area of forest land (Cunia 1965). With an increased importance placed on precise estimation of AGB for broader scales comes an increased need to accurately portray the true magnitude of their associated uncertainties. This would involve accounting for all three of the aforementioned sources of uncertainty when constructing reliability statements for AGB, rather than only the third listed source, as is usual in many broad-scale forest inventory operations. One of the primary investigations in this study aims to compare the total propagated error for two sets of regional-level AGB component equations by accounting for all three of these sources of error. This information would provide a means for determining which model is more precise for use within the region for

which they were developed, while also illustrating the relative contributions of each error type.

One additional benefit of accounting for all three sources of uncertainty is that it provides an opportunity to observe possible gains in precision to be had by addressing uncertainty that arises due to issues with tree-level explanatory measurement data. More commonly referred to as measurement error, this form of uncertainty can be addressed prior to data collection in a number of different ways. These include choice of instrument, calibration of said instrument and by minimizing faulty collection results from data observing and recording personnel through various standardized training and implementation procedures (Weiskittel et al. 2011, p.277). One of the other primary investigations in this study looks comparing the choice of high-precision instruments for addressing error propagation due to measurement error.

Terrestrial LiDAR is one such high-precision instrument that has proven useful in forest inventory applications. Terrestrial laser scanning (TLS) technology has been used for measuring tree-level metrics such as diameters outside bark and bole heights (Somonse et al. 2003, Hopkinson et al. 2004, Henning and Radtke 2006, Bienert et al. 2006, Maas et al. 2008, Weiß 2009, Pueschel et al. 2013) as well as crown metrics such as height to crown base and crown volume (Chasmer at al. 2006, Jung et al. 2011). Almost all of these studies have assessed the performance of the TLS for extracting tree-level metrics. However, no research efforts exist that have taken this information and subsequently assessed the impact of this measurement performance on the uncertainty of broad-scale estimates of forest-related parameters, such as AGB.

With this information, forest managers would also be equipped with the ability to gauge whether the gains in precision justify the investment in this technology as a tool for use in their forest inventories.

With the comparison of the total uncertainty between equations this thesis aims to illustrate the effect of accounting for all three sources of error and their relative contributions to estimates of AGB from both sets of equations. In doing so, it is shown how additional credibility can be gained for the reliability statements that accompany estimates of AGB. Additionally, this thesis also aims to show how this approach captures the impact terrestrial LiDAR can have on the precision of broad-scale AGB estimates. Chapter 2 assesses the relative contributions of all three sources of error to the total propagated error for two sets of component equations for lodgepole pine in the Pacific Northwest region. Chapter 3 compares the total propagated error associated with using the TLS versus traditional inventory instruments. Lastly, the final Chapter 4 provides a generalized synthesis of the central research findings, linking their utility into inventory and monitoring of AGB, while also tying their relevance into future research efforts that would further the efforts documented here.

CHAPTER 2: COMPARISON OF UNCERTAINTY IN PER UNIT AREA ESTIMATES OF ABOVEGROUND BIOMASS FOR TWO SELECT MODEL SETS

Introduction

Increasingly central to the planning and monitoring-related goals of disciplines such as forestry and ecology, the production of defensibly precise broad-scale estimates of above ground biomass (AGB) all but requires a thorough recognition of their primary associated sources of variability. The widespread sample-based approach of acquiring these AGB estimates for forested areas typically involves applying individual-tree regression equations to trees selected within randomly selected sample plots to obtain tree-level estimates of AGB. All individual-tree estimates are then summed to obtain plot-level estimates, with all plot values subsequently averaged then expanded up to per unit area levels of ABG. The reported precision of these per unit area estimates using this approach commonly reflect only the sampling error; the variability resulting from among-plot differences in plot-level values of ABG. In addition to sampling error, two other primary sources of error have been shown to interact and propagate during the process of scaling individual-tree estimates of AGB up to per unit area levels; namely measurement error and model error (Cunia 1965). Measurement error is defined as the difference between a defined “true” value and the measured value of a given attribute. Model errors are sourced mainly from the residual variability around the model predictions and uncertainty in the parameter estimates. Because only sampling error is accounted for, uncertainty estimates for AGB are often an underestimation of the actual uncertainty. If uncertainty estimates for AGB are to

be statistically credible, accounting for all three of these error types must take place when reporting these uncertainties.

Measurement error is a source of uncertainty that has received attention in the forestry literature. A number of authors have investigated the measurement error of particular instruments used in forestry applications (Behre (1926), Bell and Gourley (1980), McRoberts et al. (1994), Williams et al. (1994), Skovsgaard et al. 1998, Plamondon (1999), Kalliovirta et al. 2004), while others have characterized the distributions of measurement errors for measured tree variables (McRoberts et al. 1994, Canavan and Hann, 2004). Work has also been done to investigate the effects of measurement error on the uncertainty of forest model predictions (Westfall and Patterson 2007, Suty et al. 2013, Berger et al. 2014). Westfall and Patterson (2007) used the two stage error distribution method, also described by Canavan and Hann (2004), to model measurement variation distributions. Using quality assurance data from 682 inventory plots implemented by the Forest Inventory and Analysis (FIA) unit of the United States Department of Agriculture (USDA) Forest Service, they were able to assess the effects of measurement variability on several volume change estimates, including ingrowth, accretion, removals and mortality. Error due to measurement variability was minimal compared to the sampling variability, with accretion being the most sensitive to systematic measurement errors. Suty et al. (2013) used Taylor series expansion and empirical comparisons between two volume growth prediction methods to illustrate the effect of introduced bias from random measurement errors to inputs for non-linear volume growth models used in the

Swedish National Forest Inventory (NFI). Similarly, Berger et al. (2014) used Taylor series expansion and Monte Carlo simulations to approximate the effects of measurement errors in four independent variables on the relative error of stem volume equations currently used in the Austrian NFI. None of these authors, however, took the next step and looked at how measurement error affected broad-scale AGB estimates.

The effects of model errors on the variability of broad-scale forest inventory estimates have also been investigated. Breidenbach et al. (2014) assessed how variability in models used by the Norwegian NFI affects biomass stock and change estimates for Norway spruce. A parametric bootstrap approach was employed to quantify the contributions of parameter estimate uncertainty, inflated model residual variance and within-plot correlation to the total uncertainty of biomass stock and change in Norway. McRoberts and Westfall (2014) used Monte Carlo simulations to examine how volume model-related variability influences broad-area estimates generated from 2,178 FIA plots across a study area in northeastern Minnesota, USA. A comparison was made of the gains using species-specific models versus coniferous/deciduous nonspecific models, calibrated from a species-specific dataset collected from 2,102 trees across 24 states of the northern and northeastern Unites States. Both of these authors found the model errors to be minimal contributors to the total uncertainty. However, neither author investigated the effects of measurement error as well.

Unfortunately, very few studies have addressed the effects of all primary sources of error on broad-scale forestry inventory estimates. Mowrer and Frayer

(1986) addressed the effects of measurement error, model error and sampling error by measuring the cumulative variance of five 10-year projections from a growth and yield model for pure even-aged clonal quaking aspen using both Taylor series expansion and Monte Carlo simulations. Gertner (1990) approximated the effect of all three sources for non-linear individual-tree volume functions used to estimate stand-level volume per acre. Chave et al (2004) examined the effects of these different sources of error using permanent plot data from the moist forests of the canal region of Panama. In addition to the three aforementioned error sources, the magnitude of uncertainty from the specific model form chosen was assessed. This study is similar in that all three forms of error were empirically compared for two different sets of component models developed for lodgepole pine (*Pinus contorta*) for use in the Pacific Northwest region. In doing so, we were able to produce credible depictions of uncertainties useful for determining which model is the most reliable for future use.

Component Ratio Method

The FIA is charged with the task of providing stock and change estimates for a large number of national-scale forest-related variables, with their estimates of AGB being drawn upon and used for a wide range of applications. Regional-level equations for small to mid-level estimation in specific regions are publicly available and used by many individuals seeking species-specific localized component estimates of AGB. However, these suites of equations often source from an array of different studies, inconsistent methodologically and in sample size, often yielding AGB estimates that differ across regions for trees of identical size and species. To address consistency

issues in estimation across regions, the national-level Jenkins equations were developed and used by FIA for national-scale estimation (Jenkins et al. 2003). Stemming from extensive meta-analysis of 2,640 published equations for component and total-tree biomass, the resultant Jenkins equations are a group of 10 generalized component and total tree biomass equations with diameter at breast height (DBH) as the only independent variable.

Reservations about the low-level of species specificity of these generalized models arose when large variations of AGB estimates were observed when applied to smaller-scale operations. This was illustrated by Zhou and Hemstrom (2009) who observed Jenkins estimates of total AGB of softwoods in the state of Oregon to be 17% greater compared to regional species-specific equations. Hence, in 2009 a new component ratio method (CRM) was proposed as the standard for nationwide AGB reporting. This method uses a combination of the component ratios from the Jenkins equations, regional bole volume equations and percent bark estimates, so as to ensure consistency with regional tree-level volume estimates (Heath et al. 2008, Woodall et al. 2010). However, despite the conformance with regional-based estimates of bole volume, the reliance on the national-scale generalized Jenkins component ratios yields the same non-specificity for regional and finer-scale applications.

A new set of species-specific CRM component equations for lodgepole pine (*Pinus contorta*) are presented here for comparing total uncertainties with those produced from the current regional equations. These new CRM equations are heretofore referred to as the CRM equations; the hybrid CRM method described in the

previously paragraph will be referred to as CRM-FIA. These new CRM equations originate from a pilot research study aimed at developing new regional-level models for AGB consistent across regions. Rather than rely on the component ratios from the Jenkins models and the current regional volume models, these equations directly predict the proportion of tree-level AGB for bole wood, bark, branch wood and foliage. With these new CRM equations for component AGB stemming from one study, rather than a host of different studies as with the current regional equations, and with the specificity for use in smaller, more localized operations, the prior stated issues with consistency, specificity and congruence are addressed. The three independent variables for these new models are DBH, total height (HT) and height to crown base (HTCB).

To evaluate the performance of these new equations relative to the current regional approach for estimating tree-level AGB for lodgepole pine, comparisons of the magnitude of the cumulative propagated error will be made between the two sets of equations. Using Monte Carlo simulations, and applying both sets of equations to cluster sample plot data associated with destructively sampled trees used for development of the new CRM models, we were able to quantify the effects of measurement and model error on the precision of per unit area estimates of AGB for both approaches.

Methods

Study locations

In order to capture regional differences in tree form, the data for this study were collected from both the Willamette National Forest (WNF) and the Deschutes National Forest (DNF) in western and central Oregon, respectively, All locations were within a mid-elevation band, with the WNF locations spanning from 1,160-1,340 meters in elevation and the DNF locations from 1,280 to 1,340 meters in elevation. The WNF locations encompassed two forest types: (1) a diverse mixed-species coniferous forest, with observed species being Douglas-fir (*Pseudotsuga menziesii*), western hemlock (*Tsuga heterophylla*), lodgepole pine, mountain hemlock (*Tsuga mertensia*na), noble fir (*Abies procera*), Engelmann spruce (*Picea engelmanii*), and western white pine (*Pinus monticola*); and (2) a homogenous coniferous forest composed of primarily lodgepole pine and with a small element of grand fir (*Abies grandis*). The DNF locations encompassed one forest type of homogenous coniferous species composition, with observed species being lodgepole pine and ponderosa pine (*Pinus ponderosa*).

Field data

For all locations, accessible sample trees were subjectively selected based upon morphological characteristics that included DBH, HT, and crown ratio (CR), as well as absence of defect or abnormalities. Efforts were taken to select sample trees either located in different forest stands types, or sufficiently distanced apart so as to avoid

issues with spatial autocorrelation. A total of 32 trees were measured over a four week period during July and August 2013. DBH, HT and CR ranged from 13.5 to 42.9 cm, 9.2 to 31.9 m and 0.30 to 0.948, respectively.

Standing- tree measurements were conducted prior to felling, with DBH being measured to nearest 0.254 cm. using a Spencer combination tape and with both HT and height to crown base (HTCB) being measured to the nearest 0.03 m. using a Trupulse Laser Rangefinder 360R. For this study, HTCB was defined as the bole height of the first live limb. Downed-tree measurements of HT and HTCB were measured with a 30.48 m open reel fiberglass tape. Due to the need for determining the point on the bole where 4.5 ft. above the uphill side of the tree was located prior to felling, and because DBH was measured with strict attention to detail while the sample trees still stood, standing-tree measurements of DBH were considered to be the "true" values and were not subsequently re-measured. It should also be noted that a large number of additional measurements that weren't independent variables into the models were taken on the felled trees for the creation of the new CRM equations.

For estimation of component biomass per unit area, ground plot data was collected from the forest stands from which the 32 sample trees were sourced. All trees (> 4" in diameter) within a cluster plot comprised of four circular fixed area subplots arranged around each sample tree were measured for attributes such as species, DBH, HT and HTCB, among others. A 0.017 hectare plot was the primary subplot (radius 7.33 m) with the pith of the sample tree as the center. The centers of the other three circular subplots were located 36.58 m. at azimuths of 120, 240 and

360° from the pith of the sample tree. The secondary subplots were 0.008 hectares in area (radius 5.18 m), this reduction in plot size being a reflection of the relative importance of these plots to the central goal of maximizing the number of trees sampled.

Models Compared

The Pacific Northwest unit of the FIA currently uses three different equations for bole, bark and branch AGB, and a published wood specific gravity value (USDS FS 1999) to estimate lodgepole pine component AGB for region-specific applications (Zhou and Hemstrom 2010). The summation of all three component estimates of AGB is the total tree estimate of AGB, without foliage. Bole AGB for lodgepole pine is estimated by first predicting total bole wood volume using the following equation published by Brackett (1977):

$$\mathrm{CVTS}_i = 10^{-2.615591+1.847504 \times \log(DBH_i)+1.085772 \times \log(HT_i)} \quad (1)$$

where CVTS_i is the predicted total main bole wood volume including top and stump (ft^3) and log(.) is the logarithm function (base 10). This prediction is then multiplied by the following species-specific average wood density value to obtain bole AGB:

$$\text{Bole AGB}_i = \mathrm{CVTS}_i \times \mathrm{WD} \quad (2)$$

with

$$WD = SG \times W \quad (3)$$

where Bole AGB_i is the predicted the oven-dry bole biomass (lbs) for the i^{th} tree, WD is the calculated wood density value (lbs/ft³), SG is the published wood specific gravity value for lodgepole pine (0.38) and W is the density of water (62.4lbs/ft³).

Bark and branch AGB for lodgepole pine are estimated by using the following equations published by Standish (1985):

$$\text{Bark } AGB_i = 3.2+9.1\times \left(\frac{DBH_{cm,i}}{100}\right)^2 \times HT_{m,i} \quad (4)$$

$$\text{Branch } AGB_i = 7.8+12.3\times \left(\frac{DBH_{cm,i}}{100}\right)^2 \times HT_{m,i} \quad (5)$$

where Bark AGB_i is the predicted oven-dry bark biomass for the standing tree bole up to a 2.5 cm bole diameter (kg) for the i^{th} tree, Branch AGB_i is the predicted oven-dry branch biomass of wood and bark of live limbs attached to the main bole (kg) for the i^{th} tree, $DBH_{cm,i}$ is diameter at breast height (cm) and $HT_{m,i}$ is total tree height (m).

The new CRM equations under comparison here directly predict the proportion of AGB for the bole, bark, branch and foliage components. These proportions can then be multiplied by an estimate for total tree AGB of the user's choice. In this study, the total tree biomass equation used was produced using the same data used to create the CRM equations for lodgepole pine. Both the CRM equations and the total tree biomass equation were fit in separate systems of equations using the seemingly

unrelated regression method (SUR) in SAS statistical software (SAS Institute Inc., v9.4). According to Poudel (2014, personal communication)[1] the four CRM component equations and the total tree equation are of the form:

$$\text{pBole}_i=\exp[\beta_0+\beta_1\times \ln(DBH_i)+\beta_2\times \ln(HT_I)+\frac{\sigma^2}{2}] \quad (6)$$

$$\text{pBark}_i=\exp[\beta_3+\beta_4\times \ln(DBH_i)+\frac{\beta_5}{\ln(HTCB_i)}+\frac{\sigma^2}{2}] \quad (7)$$

$$\text{pBracnh}_i=\exp[\beta_6+\beta_7\times \ln(DBH_i)+\beta_8\times \ln(HTCB_i)+\frac{\sigma^2}{2}] \quad (8)$$

$$\text{pFoliage}_i=\exp[\beta_9+\beta_{10}\times \ln(DBH_i)+\beta_{11}\times \ln(HTCB_i)+\frac{\sigma^2}{2}] \quad (9)$$

$$\text{Total Tree}_i=\exp[\beta_{12}+\frac{\beta_{13}}{DBH_i}+\frac{\sigma^2}{2}] \quad (10)$$

where pBole_i, pBark_i, pBracnh_i and pFoliage_i are the estimated proportions of component AGB for bole wood, bark, branches and foliage, respectively, exp(.) is the exponential function, ln(.) is the natural logarithm function and the βs are the estimates parameters from the SUR procedure. The $\frac{\sigma^2}{2}$ is the correction factor, as described by Baskerville (1972) and McRoberts and Westfall (2014), for the resulting bias when back-transforming model predictions from the logarithmic to the initial scale of interest, where $\hat{\sigma}^2$ is the estimated mean squared error, or residual variance. In the above equations, the values of the $\hat{\beta}$s and $\hat{\sigma}^2$ are expressed on the logarithmic

[1] Poudel, K.P., Dissertation in progress. Department of Forest Engineering Resources and Management, College of Forestry, Oregon State University.

scale. For ease of future readability, all models, whether CRM, Total Tree or current regional models will be generally referred to as component models, unless where the mentioning of a specific model is deemed necessary.

Measurement Error Variability

For HT and HTCB, the differences between the standing-tree measurements and the downed-tree measurements were calculated for all 32 trees. In this study, the downed-tree measurements are considered to be the known "true" values due to the ease with which measurements could be taken as accurately as possible. The summary data for these differences were subsequently calculated for each input variable for the models (Table 2.1).

Using a grouping method detailed by Hosmer and Lemeshow (1989), and implemented by Berger et al. (2014), a simple linear regression model through the origin was constructed to predict the standard deviation of the measurement errors. In order to conduct regressions of standard deviation of measurement errors on input variables, the data required grouping. Using the notation and general methodology of Berger et al (2014) for the example of HT: (1) the data were sorted in ascending order with respect to downed-tree measurement HT values; (2) with the minimum 10 groups, as recommended by Hosmer and Lemeshow (1989), the sorted HT values were grouped into groups of size 3, with the last group including the remainder of the HT values; (3) for every g^{th} group, the means of the HT measurements from step 1 and $SD_{ME,g}$ were estimated, where $SD_{ME,g} = \frac{1}{n-1}\sqrt{\sum_{g=1}^{n}\left(ME_{HT.g} - \overline{ME_{HT.g}}\right)^2}$ is the

standard deviation of the measurement errors for HT and $ME_{HT,g} = HT_D\text{-}HT_S$ are the HT measurement errors, where HT_D is the downed-tree height measurement and HT_S is the standing-tree height measurement; (4) the following model form was fit to the grouped data for HT using the method of ordinary least squares:

$$\widehat{SD}_{ME,HT}=\hat{\beta}_1 \times HT \tag{11}$$

where $\widehat{SD}_{ME,HT}$ is the estimated standard deviation of the measurement errors for *HT* and $\hat{\beta}_1$ is the model parameter estimate.

Integrating Simulated Measurement Errors into Model Uncertainty

We based our methods of integrating the measurement error into the model uncertainty on those described by Berger et al. (2014). Using the standard deviations from Table 2.1 and equation 11, Monte Carlo simulations, conducted using R software (R Core Team 2012), were used to approximate model uncertainties reflective of the additional uncertainty due to measurement error. Within each simulation, we were able to produce measurement errors that were then applied to "true" input values from the downed-tree measurements to produce "contaminated" input values for the equations. Input variable contamination was a two part process. For consistency, we will stay with the example of HT. First, for the k^{th} component model, a multiplicative factor ~N(1, SD_{HT}^2) was randomly generated and multiplied together with the input variables, where SD_{HT} is the standard deviation of the height measurement errors in Table 2.1; and (2) an additive factor ~N(0, $\widehat{SD}_{ME,HT}^2$) was randomly generated and

added to the input variables, where $\widehat{SD}_{ME,HT}$ is the predicted standard deviation from equation 11 (Berger et al. 2014).

The resultant contaminated model predictions were recorded over 5000 iterations, for all component models. The impact of the additional uncertainty was assessed by calculating the mean prediction and root mean square error (RMSE) and the relative RMSE (RRMSE) over all iterations using the dataset of 32 trees with the following formulas:

$$\text{mean} = \frac{1}{n}\sum_{i=1}^{n} \hat{Y}_i \tag{12}$$

$$\text{RMSE} = \sqrt{\frac{1}{n}\sum_{i=1}^{n}\left(Y_i - \hat{Y}_i\right)^2} \tag{13}$$

where Y_i is the observed value and $\widehat{Y}_i$ is the prediction for the i^{th} tree. RRMSE is calculated by simply dividing RMSE by the mean.

To convert the CRM predicted ratios and RMSEs to tree-level units (oven-dry kg), two steps were taken; (1) the CRM ratios were multiplied by the prediction for total tree biomass produced by equation 10 to obtain tree-level predictions of component AGB; (2) to produce absolute RMSEs for this product, the square root of the sum of the squared relative RMSEs was multiplied by the predictions in step 1. The following formula for the combined RMSEs is

$$\delta AGB_{Comp} = \widehat{AGB}_{Comp} \times \sqrt{\left(\frac{\delta AGB_{Ratio}}{\widehat{AGB}_{Ratio}}\right)^2 + \left(\frac{\delta AGB_{TT}}{\widehat{AGB}_{TT}}\right)^2} \qquad (14)$$

where δAGB_{Comp} is the combined RMSE in tree-level units, δAGB_{Ratio} is the RMSE for the CRM component ratios and δAGB_{TT} is the RMSE for Total Tree AGB (equation 10).

Integrating Models Errors into Sampling Uncertainty

In order to integrate the model errors, contaminated or not, into the sampling uncertainty, the magnitude of the model errors integrated needed to be contingent upon the magnitude of the model predictions. Using the previously described grouping approach with respect to the model errors, a simple linear regression model through the origin was constructed to predict the magnitude of the model errors. Following the notation and general methodology of McRoberts and Wesfall (2014): (1) for the k^{th} component model, a joined list of ε_i, Y_i and $\hat{Y}_i$ was created and sorted in ascending order with respect to $\hat{Y}_i$, where $\varepsilon_i = \hat{Y}_i - Y_i$; (2) with the minimum 10 groups, as recommended by Hosmer and Lemeshow (1989), the sorted triads of observations were grouped into groups of size 3, with the last group including the remainder of the means; (3) for every g^{th} group, the mean observation $\bar{Y}_g = \frac{1}{n_g}\sum_{g=1}^{n_g} Y_g$, the mean prediction $\overline{\hat{Y}_g} = \frac{1}{n_g}\sum_{g=1}^{n_g} \hat{Y}_g$ and the mean square error $\sigma_g^2 = \frac{1}{n_g - 1}\sum_{g=1}^{n} \varepsilon_g^2$ were calculated, where n_g is the number of trees in the g^{th} group; (4) the following model

form was fit to the grouped data for each component model using the method of ordinary least squares

$$\hat{\sigma}_i=\hat{\beta}_1*\hat{Y}_i \quad (15)$$

where $\hat{\sigma}_i$ is the predicted model error for the i^{th} tree, $\hat{\beta}_1$ is the model parameter estimate and $\hat{Y}_i$ is the model prediction for the i^{th} tree. It should be noted that with measurement error integrated into the model errors, the value of $\hat{\beta}_1$ is expected to increase, reflecting this additionally accounted for source of uncertainty.

A bootstrapping technique, in conjunction with equation 15, was used to simulate the effects of model errors on the uncertainty of per unit area estimates of component AGB for all models. A similar Monte Carlo simulation sequence and notation described by McRoberts and Westfall (2014) was used for each component model.

First, the data set containing the "true" values of the 32 sample trees was randomly sampled with replacement to produce a bootstrapped-sample of size 32. Similar to the previously described method of simulating measurement errors, contaminated model predictions for all 32 pseudo-sampled trees were produced by adding a randomly generated residual, $\varepsilon_i \sim N(0, \hat{\sigma}_i^2)$, to the prediction for the i^{th} pseudo-sampled tree produced using the k^{th} component model, where $\hat{\sigma}_i$ is estimated using equation 16. Using the contaminated predictions and the pseudo sample data, a new model, of the same form as the k^{th} component model, was refit. For equations 1, 6, 7, 8, 9 and 10, due to their original model form, the contaminated predictions and

the pseudo sample data required transformation to the $\log_{10}$-$\log_{10}$ and ln-ln scale, respectively, prior to refitting.

Second, the refit equations were applied to the ground plot data set. For the i^{th} tree in the j^{th} plot, predictions of tree-level component AGB were produced by adding the model predictions to a randomly generated constrained residual, $\lambda\varepsilon_i$ where ε_i is the randomly generated residual ~N(0, $\hat{\sigma}_i^2$), and λ is a multiplicative constraining factor that yields model efficiency values of 0.95. Model efficiency, calculated as

$$Q^2 = 1 - \left(\frac{\sum_{i=1}^{n_{pl}} e_i^2}{\sum_{i=1}^{n_{pl}} (Y_i - \overline{Y})^2} \right) \qquad (16)$$

where n_{pl} is the number of trees in the ground plot data set, is a goodness-of-fit statistic similar to the more familiar r^2 from the ordinary least squares procedure, where the higher the value the better the fit of the model to a given data set (Vanclay and Skovsgaard 1997, McRoberts and Westfall 2014). This multiplicative factor constraint was implemented in order to have a standardized quality of fit of the model to the ground plot data for purposes of comparing the standard errors of the mean for all component models. Due to recent published findings illustrating the minimal effect correlation among trees within plots has on the standard error of the estimates, correlation among residuals was not integrated into the analysis of this study (Berger et al. 2014, Breidenbach et al. 2014, McRoberts et al. 2014).

Third, to obtain the estimated per acre values of component AGB on the j^{th} cluster plot, the summation of all subplot-level per unit area component AGB predictions on the l^{th} subplot were calculated as

$$Y_j = \sum_{l=1}^{4} Y_l \tag{17}$$

with

$$Y_l = \frac{\sum_{l=1}^{n_j} Y_{i,l}}{Subplot\ Area_{hectares}} \tag{18}$$

where n_l is the number of trees observed in the l^{th} subplot and $Y_{i,l}$ is the i^{th} tree on the l^{th} subplot.

Fourth, for each simulation cycle the mean and variance of the mean across all cluster plots were calculated as

$$\bar{Y} = \frac{1}{n_{cl}} \sum_{j=1}^{n_{cl}} Y_j \tag{19}$$

$$\widehat{\mathrm{Var}}(\bar{Y}) = \frac{1}{n_{cl}(n_{cl}-1)} \sum_{j=1}^{n_{cl}} (Y_j - \bar{Y})^2 \tag{20}$$

where n_{cl} is the number of cluster plots (32 in this study).

Finally, the mean prediction and mean within-simulation variance over 5000 simulation cycles were calculated as

$$\hat{\mu}_{sim} = \frac{1}{5000}\sum_{1}^{5000} \bar{Y} \quad (21)$$

$$\widehat{\mathrm{Var}}_{sim} = \frac{1}{5000}\sum_{1}^{5000} \widehat{\mathrm{Var}}(\bar{Y}) \quad (22)$$

Comparisons of the mean predictions as well as final propagated error will be compared for all component models for both approaches. Metrics used for comparison include RMSE, RRMSE, standard error of the mean (SE) from equation 20 and relative SE (RSE).

Results and Discussion

Model Predictions and Uncertainty

Once the predicted CRM component ratios were produced, they were multiplied by the predicted total tree biomass obtained using the SUR equation. When measurement error is not integrated into the model errors, the CRM predicts comparable amounts of tree-level AGB for each component, except for branches where the CRM predicts over 2.5 times that of the currently used Standish (1985) equations (Table 2.2). This difference could likely be explained by differences between the geographic location of the two study locations, as well as differences in the field protocol for sub-sampling branches. The Standish (1985) equations were fit from a dataset stemming from throughout the province of British Columbia, Canada where a difference in growing season duration and conditions may result in less branch AGB than in the mid latitudes of lodgepole pines range, where the data in this

study are sourced. The sub-sampled branches selected in the Standish (1985) study were randomly selected from three diameter classes, two from each class, whereas in this study branches were randomly selected, independent of size, from three different live crown height strata, with four from the bottom, three from the middle and two from the top stratum, giving greater weight to the portion of the crown where larger branches typically occur. As a result of this difference in predicted branch AGB, the predicted total tree AGB without foliage (TTWOF) when measurement error is not accounted for is greater than that of the regional equations. This result contrasts to the results found by Chojnacky (2012) who found the aforementioned hybrid CRM approach to yield predictions that were less than those from the current regional suite of equations for all but two genera. RMSE values for tree-level component and TTWOF estimates were generally larger for the regional models, with the RMSE for the regional bole and branch component models being 53% and 41% higher, respectively, than the CRM component model RMSEs. The TTWOF RMSE for the regional estimate was also 45% higher than the CRM estimate.

With the integration of measurement error into the model errors, this difference between TTWOF RMSE values was substantially larger (Table 2.3). As expected, all RMSE values increased for all tree-level component and TTWOF RMSE values, but the 621% increase from 79.56 kg without measurement error to 573.95 kg with measurement error for the regional bole component model RMSE was dramatic. RRMSE values for all regional models showed substantial increase as well (Table 2.4). This substantial imprecision is most likely due to extrapolation, which occurred

through the random simulation of measurement errors. The measurement error simulation procedure produced intermittently extreme values of DBH and HT for inputs into the equation. Hence, this dramatic increase illustrates the model not being suitable for extrapolation outside the range of DBH and HT for which it was intended. With the TTWOF RMSE value for the regional equations being almost five times that of the CRM TTWOF RMSE value, the CRM was the more precise approach for tree level estimation of AGB. The model prediction for the regional bole component model also increased a substantial 86% with simulated measurement error integrated, resulting in a 72% increase for TTWOF. The CRM model predictions for branch and foliage AGB increased slightly, while the predictions for bole and bark AGB decreased with simulated measurement error, resulting in a 7% decrease for TTWOF for the CRM prediction.

Per Unit Area Estimates and Uncertainty

When only sampling error is considered for per unit area estimation, the standard error of the means for the CRM were greater in magnitude than those produced using the current regional equations (Table 2.5), showing a reversal in the trend observed with the model RMSEs. However, the RSEs are very comparable; particularly the TTWOF RSE values (Table 2.7). As was the case with the tree-level predictions, the bole and branch component models comprise the two greatest portions of the TTWOF variability, with the CRM branch model precision being substantially less than the regional branch model. This relatively large TTWOF RSE value can likely be attributed to three reasons relating to the ground plot data. First, the small

plot sizes of the three outer 1/48th acre subplots likely reduced the precision of the per acre estimates of component AGB (Johnson and Hixon 1952, Freese 1961, Gray 2003). Secondly, the ground plot data was combined from different forest locations, with different species compositions, stand densities and structure. Thus, the variability between the 32 cluster plots was expectedly large. Third, the small sample size of only 32 cluster plots could be contributing to these large RSE values as well. Similar to the tree-level predictions when measurement error integrated, the CRM predictions for all components and TTWOF were larger than those produced by the regional equations.

When the model error was integrated into the simulations for per unit area estimation, the precision of the current regional equation predictions was relatively unchanged; showing less than a 2% increase in the SE for TTWOF, suggesting the model error of the regional models are trivial contributors to the total uncertainty (Table 2.6). This is in line with the results of several authors who have looked at the effects of model uncertainty on per unit area estimates of forestry parameters (Berger et al. 2014, Breidenbach et al. 2014, McRoberts and Westfall 2014, Ståhl et al. 2014). With the relatively small sample size of only 32 trees, this small increase in uncertainty could partially be attributed to the Q^2=0.95 constraint for establishing a baseline of comparison between the two sets of equations. However, we anticipate the SE values would only marginally increase without this constraint, as shown by McRoberts and Westfall (2014).

The precision of the CRM predictions, however, showed a substantial change with integration of model errors, with the SE for TTWOF increasing nearly threefold.

With the CRM approach, where two estimates with their own amounts of uncertainty are multiplied together, the resulting estimate of total component AGB is hierarchical in nature; with the residuals of the Total Tree and component ratio equations being serially correlated. When this degree of serial correlation is present between the residuals of two hierarchical responses, predictions themselves will be unbiased and consistent, but will also be highly inefficient with the uncertainty estimates being enlarged (Kutner et al. 2004, p.481). Thus, as suggested by the results of the simulations in this study, the effect of applying both CRM estimates to plot data and multiplying the resultant estimates together, without accounting for the correlation structure between these two models, can produce per unit area estimates with a low degree of reliability.

The effect of accounting for measurement error in addition to model and sampling error was seen in an increase in the SE and RSE values for both sets of equations (Tables 2.7 & 2.8). The TTWOF SE for the CRM and regional equations increased by 15% and 5%, respectively. The relative proportions of SE due to measurement, model and sampling error for the regional equations were 5%, 2% and 93%, respectively. Gertner (1990) found similar results for proportion of total variance while looking at the effect of all three sources of error while estimating stand-level volume per acre. The same relative proportions of SE for the CRM equations were 13%, 55% and 32%, for measurement, model and sampling error, respectively. The relative proportion of the SE due to measurement error being as large as it is (13%)

indicates the measurement error also contributed fairly heavily to the total per unit area uncertainty for the CRM estimates.

With a relatively small dataset of only 32 lodgepole pine trees that were subjectively selected, rather than probabilistically, from a fairly limited portion of the species' range, the predictions and their respective uncertainties reported in this study likely have amount of bias. However, despite these admitted inferential limits, a clear depiction of the general contributions of measurement, model and sampling error to the total propagated error was given for both models.

Conclusion

As defensibly precise estimates of AGB across a range of scales are increasingly sought after by FIA and others users of individual-tree biomass equations, the need to produce reliable depictions of their associated uncertainty will continue to develop. This study has confirmed that not accounting for both measurement and model error does in fact result in an underestimation of per unit area uncertainty of AGB. Due to the substantial contribution of the models errors with the CRM equations, the per unit area estimates produced with those equations were much less precise than the current regional equations.

Ultimately, if FIA were to implement the usage of these CRM equations for lodgepole pine in the Pacific Northwest region, accounting for the uncertainty of the combined equations should accompany this implementation. This would result in reliability statements with increased credibility. While the predicted means from the

CRM equations could theoretically yield more accurate estimates when applied to different stands of lodgepole pine, the results of this study suggest those estimates would be less precise than those that would be produced by the current regional equations. The results of this study also provide an impetus for future research to depict the anticipated reduction in uncertainty associated with accounting for the aforementioned correlation structure. Further, given these results it is reasonable to assume the precision of the estimates produced by the CRM-FIA approach are substantially underestimated. While the issue of consistency with the current regional models is still prevalent, the comparatively greater reliability of their estimates of AGB on a per unit area basis, using the trees in this study, dissuades their replacement for small to midscale usage by the CRM equations evaluated here.

References

Baskerville, G.L. 1972. Use of logarithmic regression in the estimation of plant biomass. Can. J. of For. Res. 2(1):49-53

Behre, C.E. 1926. Comparison of diameter tape and caliper measurements in second-growth spruce. J. Forestry., 24(2):178-182

Berger. A., Gschwantner, R.E., McRoberts, R.E., and Schadauer, K. 2014. Effects of measurement errors on individual tree stem volume estimates for the Austrian National Forest Inventory. For. Sci. 60(1):14-24

Bell, J.F., and Gourley, R. 1980. Assessing the accuracy of a sectional pole, Haga altimeter, and alti-level for determining total height of young coniferous stands. South. J. of App. For. 4(3):136-138

Brackett, M. 1977. Note on TARIF tree-volume computation. DNR Rep. 24. Olympia, WA: Washington Department of Natural Resources. 132p

Breidenbach, J., Antón-Fernández, C., Petersson H., Astrup, P., and McRoberts, R.E. 2014. Quantifying the model-related variability of biomass stock and change estimates in the Norwegian National Forest Inventory. For. Sci. 60(1):25-33

Canavan, S.J., and Hann, D.W. 2004. The two-stage method for measurement error characterization. For. Sci. 50(6):743-756

Chave, J., Condit, R., Aguilar, S., Hernandez, A., Lao, S., and Perez, R. 2004. Error propagation and scaling in tropical forest biomass estimates. Philos. Trans. R. Soc. Lond. B 359(1443):409:420

Chojnacky, David C. 2012. FIA's volume-to-biomass conversion method (CRM) generally underestimates biomass in comparison to published equations. Moving from Status to Trends: Forest Inventory and Analysis (FIA) Symposium 2012, pp. 396-402. GTR-NRS- P-105. US Department of Agriculture, Forest Service, Northern Research Station.

Cunia, T. 1965. Some theory on reliability of volume estimates in a forest inventory sample. For. Sci., 11(1):115-128.

Forest Products Laboratory. 2010. Wood handbook—Wood as an engineering material. Gen. Tech. Rep. FPL-GTR-190. Madison, WI: U.S. Department of Agriculture, Forest Service, Forest Products Laboratory. 508 p

Freese, F., 1961.Relation of plot size to variability: an approximation. J. Forestry. 59:679

Gertner, G.Z. 1990. The sensitivity of measurement error in stand volume estimation. Can. J. of For. Res. 20(6):800-804

Gray, A. 2003. Monitoring stand structure in mature coastal Douglas-fir forests: effect of plot size. For. Ecol. Manage., 175(1):1-16.

Heath, L.S., M.H. Hansen, J.E. Smith, W.B. Smith, and P.D. Miles. 2008. Investigation into calculating tree biomass and carbon in the FIADB using a biomass expansion factor approach. In: McWilliams, W.; Moisen, G.; Czaplewski, R., comps. 208 Forest Inventory and Analysis (FIA) symposium. Proc. RMRS-P-56 CD. Fort Collins, CO: U.S. Department of Agriculture, Forest Service, Rocky Mountain Research Station. [CD–ROM].

Hosmer, D.W., and Lemeshow, S. 1989. Applied Logistic Regression. New York: John Wiley & Sons, Inc. 307p

Jenkins, J.C., Chojnacky, D.C., Heath, L.S., and Birdsey, R.A. 2003. National-scale biomass estimators for United States tree species. For. Sci. 49(1):12.-35

Johnson, F.A., and Hixon, H.J., 1952. The most efficient size and shape of plot to use for cruising in old-growth Douglas-fir timber. J. For. 50(1):17-20

Kalliovirta, J., Laasasenaho, J., and Kangas, A. 2004. Evaluation of the laser-relaskop. For. Ecol. Manage. 204:171-194

Kutner, M.H., Nachtsheim, C.J., and Neter, J. 2004. Applied Linear Regression Models. McGraw-Hill/Irwin.

McRoberts, R.E., Hahn, J.T., Hefty G.J., and Van Cleve, J.R. 1994. Variation in forest inventory field measurements. Can. J. For. Res. 24:1766-1770.

McRoberts, R.E., and Westfall, J.A. 2014. Effects of uncertainty in model predictions of individual tree volume on large area volume estimates. For. Sci. 60(1):34-42

Mowrer, H.T., and Frayer, W.E. 1986. Variance propagation in growth and yield projections. Can. J. of For. Res. 16(6):1196-1200

Plamondon, J. A. 1999. Log-length measurement errors with six single-grip harvester heads. Technical Note Forest Engineering Research Institute of Canada - FERIC, No. TN-297. 6p.

R Core Team (2012). R: A language and environment for statistical computing. R Foundation for Statistical Computing, Vienna, Austria. ISBN 3-900051-07-0, URL http://www.Rproject.org/

SAS Institute Inc. Output for this paper was generated using SAS software, Version 9.4 of the SAS System for Windows. Copyright © 2013 SAS Institute Inc. SAS and all other SAS Institute Inc. product or service names are registered trademarks or trademarks of SAS Institute Inc., Cary, NC, USA.

Skovsgaard, J.P., Johannsen, V.K., and Vanclay, J.K. 1998. Accuracy and precision of two laser dendrometers. Forestry 71:131-139

Ståhl, G., Heikkinen, J., Petersson, H., Repola, J., and Holm, S. 2014. Sample-based estimation of greenhouse gas emissions from forests-a new approach to account for both sampling and model errors.

Standish, J.T., Manning, G.H., and Demaerschalk, J.P. 1985. Development of biomass equations for British Columbia tree species. Information Report BC-X-264. Canadian Forest Service, Pacific Resource Center. 47p

Suty, N., Nyström, K., and Ståhl, G. (2013). Assessment of bias due to random measurement errors in stem volume growth estimation by the Swedish National Forest Inventory. Scand. J.of For.Res.28(2), 174-183.

Vanclay, J.K., Skovsgaard, J.P. 1997. Evaluating forest growth models. Ecol. Model. 98(1):1-12

Wesfall, J.A., and Patterson, P.L. 2007. Measurement variability error for estimates of volume change. Can J. of For. 37(11):2201-2210

Williams, M.S., Bechtold, W.A., and LaBau, V.J. 1994. Five instruments for measuring tree height: An evaluation. South. J. App. For. 18(2):76-82.

Woodall, C.W., Heath, L.S., Domke, G.M., and Nichols, M.C. 2011. Methods and equations for estimating aboveground volume, biomass, and carbon for trees in the U.S. forest inventory, 2010. Gen. Tech. Rep. NRS-88. Newton Square, PA: U.S. Department of Agriculture, Forest Service, Northern Research Station. 30p

Zhou, X. P., and Hemstrom, M. A. 2009. Estimating aboveground tree biomass on forest land in the Pacific Northwest: a comparison of approaches. Res. Pap. PNW-RP-584. Portland, OR: U.S. Department of Agriculture, Forest Service, Pacific Northwest Research Station. 18p

Zhou, X. P., and Hemstrom, M. A. 2010. Timber volume and aboveground live tree biomass estimations for landscape analyses in the Pacific Northwest. Gen. Tech. Rep. PNW-GTR- 819. Portland, OR: U.S. Department of Agriculture, Forest Service, Pacific Northwest Research Station. 31 p

Table 2.1: Summary statistics of the measurements errors for HT and HTCB

	n	Min.	Mean	Max.	SD
HT (m)	32	-2.56	-0.82	2.26	0.83
HTCB (m)	32	-1.04	-0.07	1.37	0.49

Table 2.2: Model predictions and RMSE values for CRM ratios, CRM tree-level estimates and tree-level estimates for the regional equations, without measurement error. Total minus foliage, the sum of the tree-level component estimates, is used as another means for comparison between the models. Tree-levels units are in kilograms of dry biomass.

Model Means-Without Measurement Error				**Model RMSEs-Without Measurement Error**			
Total Tree (SUR)	284.83			**Total Tree (SUR)**	73.78		
Component	**CRM Ratios**	**CRM Tree-Level**	**Regional Tree-Level**	**Component**	**CRM Ratios**	**CRM Tree-Level**	**Regional Tree-Level**
Bole	0.677	192.83	182.44	**Bole**	0.081	55.04	79.56
Bark	0.054	15.42	14.21	**Bark**	0.031	9.76	10.59
Branch	0.192	54.79	20.78	**Branch**	0.061	22.34	30.74
Foliage	0.080	22.69	NA	**Foliage**	0.023	8.81	NA
Total Minus Foliage		263.04	217.43	**Total Minus Foliage**		87.14	120.89

Table 2.3: Model predictions and RMSE values for CRM ratios, CRM tree-level estimates and tree-level estimates for the regional equations, with measurement error. Total minus foliage, the sum of the tree-level component estimates, is used as another means for comparison between the models. Tree-levels units are in kilograms of dry biomass.

Model Means-With Measurement Error				Model RMSEs-With Measurement Error			
Total Tree (SUR)	284.83			**Total Tree (SUR)**	73.78		
Component	**CRM Ratios**	**CRM Tree-Level**	**Regional Tree-Level**	**Component**	**CRM Ratios**	**CRM Tree-Level**	**Regional Tree-Level**
Bole	0.607	172.92	338.50	**Bole**	0.324	157.07	573.95
Bark	0.044	12.40	14.13	**Bark**	0.057	16.62	49.99
Branch	0.207	58.93	20.67	**Branch**	0.079	27.22	72.87
Foliage	0.090	25.52	NA	**Foliage**	0.040	13.07	NA
Total Minus Foliage		244.24	373.29	**Total Minus Foliage**		200.91	696.80

Table 2.4: Model RRMSE values for CRM ratios, CRM tree-level estimates and tree-level estimates for the regional equations, with and without measurement error. Total minus foliage, the sum of the tree-level component estimates, is used as another means for comparison between the models.

Model RRMSEs-Without Measurement Error				Model RRMSEs-With Measurement Error			
Total Tree (SUR)	24.1%						
Component	**CRM Ratios**	**CRM Tree-Level**	**Regional Tree-Level**	**Component**	**CRM Ratios**	**CRM Tree-Level**	**Regional Tree-Level**
Bole	12.0%	28.5%	43.6%	**Bole**	53.4%	77.5%	169.6%
Bark	57.7%	63.3%	74.5%	**Bark**	131.6%	155.7%	353.9%
Branch	31.5%	40.8%	147.9%	**Branch**	38.2%	62.4%	352.6%
Foliage	28.9%	38.8%	NA	**Foliage**	44.2%	68.3%	NA
Total Minus Foliage		42.9%	55.6%	**Total Minus Foliage**		77.8%	186.7%

Table 2.5: Per hectare estimates and SE values for CRM and regional equations, without accounting for measurement or model error. Total minus foliage, the sum of the per acre component estimates, is used as another means for comparison between the models. Tree-levels units are in kilograms of dry biomass per hectare.

Sampling Error Only					
	Mean			SE	
Component	CRM Plot-Level	Regional Plot-Level	Component	CRM Plot-Level	Regional Plot-Level
Bole	24690.09	17875.77	**Bole**	4373.71	3383.30
Bark	1862.87	1578.96	**Bark**	330.47	284.07
Branch	6489.43	2497.86	**Branch**	1130.67	436.49
Foliage	2603.83	NA	**Foliage**	438.48	NA
Total Minus Foliage	**33042.39**	21952.59	**Total Minus Foliage**	5834.85	4103.86

Table 2.6: Per hectare estimates and SE values for CRM and regional equations, accounting for model error. Total minus foliage, the sum of the per acre component estimates, is used as another means for comparison between the models. Tree-levels units are in kilograms of dry biomass per hectare.

Sampling Error (With Model Error)					
	Mean			SE	
Component	CRM Plot-Level	Regional Plot-Level	Component	CRM Plot-Level	Regional Plot-Level
Bole	32768.33	16940.20	**Bole**	11649.73	3341.45
Bark	3253.51	1602.48	**Bark**	1253.84	295.64
Branch	9896.37	2971.86	**Branch**	3130.85	548.02
Foliage	3109.95	NA	**Foliage**	742.51	NA
Total Minus Foliage	**45918.20**	**21514.55**	**Total Minus Foliage**	16034.43	4185.12

Table 2.7: Per hectare estimates and SE values for CRM and regional equations, accounting for both measurement and model error. Total minus foliage, the sum of the per acre component estimates, is used as another means for comparison between the models. Tree-levels units are in kilograms of dry biomass per hectare.

Sampling Error (With Model and Measurement Error)					
	Mean			SE	
Component	CRM Plot-Level	Regional Plot-Level	Component	CRM Plot-Level	Regional Plot-Level
Bole	33287.96	16701.94	**Bole**	12245.38	3566.87
Bark	6673.57	1600.91	**Bark**	2893.22	296.29
Branch	10227.99	2968.04	**Branch**	3335.24	547.98
Foliage	3272.53	NA	**Foliage**	803.54	NA
Total Minus Foliage	**50189.53**	**21270.89**	**Total Minus Foliage**	18473.84	4411.13

Table 2.8: RSE values for CRM and regional equations, for all three scenarios depicted in the previous three tables. Total minus foliage, the sum of the per acre component estimates, is used as another means for comparison between the models.

Sampling Error (RSEs)						
	Sampling Only		Model Errors		Measurement and Model Errors	
Component	CRM Plot-Level	Regional Plot-Level	CRM Plot-Level	Regional Plot-Level	CRM Plot-Level	Regional Plot-Level
Bole	17.7%	18.9%	35.6%	19.7%	36.8%	21.4%
Bark	17.7%	18.0%	38.5%	18.4%	43.4%	18.5%
Branch	17.4%	17.5%	31.6%	18.4%	32.6%	18.5%
Foliage	16.8%	NA	23.9%	NA	24.6%	NA
Total Minus Foliage	18.5%	18.7%	34.9%	19.5%	36.8%	20.7%

CHAPTER 3: ADDRESSING UNCERTAINTY IN PER UNIT AREA ESTIMATES OF ABOVEGROUND BIOMASS USING TERRESTRIAL LIDAR

Introduction

Sound forest management decisions that satisfy an array of ecological, economic and social criteria are often based upon forest attributes that carry with them a defensible magnitude of certainty. Broad-scale forest inventory and monitoring programs such as the United State Department of Agriculture (USDA) Forest Inventory and Analysis (FIA) produce estimates and reports of forest resources that bear increasing utility for agencies and other users alike. The need for uncertainty statements with rigorous and thorough construct, accurately depicting the precision of the point estimates they theoretically encapsulate, is also increasing. With the growing use of FIA inventory data for attributes such as above ground biomass (AGB), gains in precision made by addressing specific sources of uncertainty could yield far-reaching benefits for forest managers, and scientists drawing inference and making decisions from their AGB estimates.

The largest source of uncertainty in a typical inventory setting is often sampling error (Mowrer and Frayer 1986, Gertner 1990), which is the uncertainty reflecting the intractability of obtaining a census on the entirety of the AGB resources in given forested area. The size of this error is contingent upon the sampling methodology and intensity and the inherent variation in the items being sampled. This is also frequently the only variability estimate accounted for when inventory reports are produced. However, based upon results discussed in Chapter 2, other sources of

uncertainty, or error, need to be addressed. Depending upon the allometric model, or sets of models, used to predict tree-level AGB, model errors tend to contribute minimally toward the total uncertainty. Measurement error, however, has been shown in previous studies, as well as in Chapter 2, to be a notably sizeable contributor to this uncertainty worthy of addressing.

Terrestrial LiDAR

When conducting a sample-based forest inventory, an array of measurements on selected sample trees are carefully taken with various instruments. Assuming rigorous calibration, the quality of instrument readings depend primarily upon ocular judgment and varying skill levels of usage. The inevitable deviation from true values of the attributes due to this inherent variability in readings can be minimized in a number of different ways. Relevant to this study, choice of instrument can have a profound impact on the magnitude of these measurement errors.

Terrestrial LiDAR technology holds promise for the addressing of measurement error through automated extraction of desired parameters. Unlike airborne laser scanning (ALS) technology, which already has wider use in broad-scale forest inventories, terrestrial laser scanning (TLS) technology emits laser light pulses at much higher point densities from a grounded perspective. This results in informationally-dense 3D geometric representations, known as point clouds, of lower to mid-vertical forest structure useful for finer-scale tree and plot-level analysis. With additional detail captured of the below-canopy architecture, foresters are able to

extract information about the vertical profile of the merchantable portion of the stem, which can be seen from below but not from above the canopy.

As opposed to being secured onto small aircraft as with ALS systems, TLS units are typically mounted and operated on tripods for use in forest inventory applications. Despite being obviously limited to smaller area applications, use of the TLS in these scenarios is applicable for isolated sample plots where the entirety of a forested land-base is not measured. With many forest inventory operations, such as FIA, using a cluster plot design, a design used in part to minimize travel costs, the spatial coverage limitation with the TLS would likely not be a prohibitive factor for its use.

Several authors have assessed the performance of TLS in obtaining specific individual-tree variables, such as taper (Thies et al. 2004), diameter outside bark (DOB) (Somonse et al. 2003, Hopkinson et al. 2004, Henning and Radtke 2006, Bienert et al. 2006, Maas et al. 2008, Weiß 2009, Pueschel et al. 2013), canopy metrics such as crown area, crown volume and height to crown base (Chasmer at al. 2006, Jung et al. 2011), and bole reconstruction for stem volume calculation (Yu et al. 2012). Henning and Radtke (2004) compared DOB measurements of nine destructively sampled loblolly pine (*Pinus taeda*) trees to DOB measurements obtained. DOBs, measured in 1m intervals, were reported to be within 1-2cm, with greater accuracy achieved for stem portions below the base of live crown. Maas et al. (2004) and Bienert et al. (2006) reviewed and compared work flow and data processing procedures for extracting common inventory attributes such as DOBs and

total tree height (HT). Chasmer et al. (2006) used coinciding ALS and TLS data to compare against field-based plot measurements of HT, height to crown base (HTCB) and maximum crown width. Average height estimate biases were similar for both ALS and TLS at 1.1m and 1.2m, respectively. ALS overestimated HTCB by an average of 1.4m due to point density distributions being weighted toward the top of the tree, whereas TLS underestimated HTCB by 6.4m, not only resulting from the inverse of the aforementioned distribution due to an inverted perspective, but largely due to not accounting for the occurrence of dead branches.

The great majority of these studies have focused primarily on investigating how tree-level TLS measurements compare to either felled or standing tree measurements. Yet, to our knowledge, no studies have been done to assess the effects of TLS measurement errors on the final uncertainty of per unit area estimate of AGB. This is relevant for broad-scale inventory and monitoring program like FIA that may benefit from using TLS for inventory measurements, where the impact of these propagated errors can be substantial when expanded to broader scales. Hence, this study investigates how the total propagated error of AGB associated with using a TLS compares to that associated with using common forest inventory instruments used for standing tree measurements. This study uses data from three types of measurements performed on 25 lodgepole pine (*Pinus contorta*) trees as the basis for making these comparisons. TLS scan data, standing tree-measurements using traditional forest inventory instruments and destructive sampling measurements comprise the three measurement sets. Using the CRM set of models for predicting lodgepole pine AGB examined in Chapter 2, the same Monte Carlo simulation approach will be employed

for making comparisons between associated uncertainties of per unit area estimates of AGB for each measurement method.

Methods

Study locations, sample tree selection criteria and procedures remain the same as described in Chapter 2. However, due to logistical circumstances limiting scanner use in the field only 25 of the 32 measured and felled trees were scanned with the TLS. Hence, for future reference the dataset used in this study contains measurements for 25 trees. For these 25 trees, true values of DBH, HT and CR ranged from 13.5 to 42.2 cm, 9.2 to 28.3 m. and 0.373 to 0.947, respectively. Details for standing tree measurement, downed-tree measurement and inventory plot protocols are also described in Chapter 2.

TLS Field Scanning Protocol

In addition to the standing tree measurements, sample trees were scanned with a tripod-mounted FARO Focus^{3D} 120 TLS prior to felling. As opposed to the more common time-of-flight TLS technology the FARO scanner uses phase shift technology which uses the shifts of modulated waves of returned infrared light pulses to calculate distances traveled (FARO 2014). Maximum ranges of phase-based scanners are less than those of time-of-flight scanners; however, measurement rates (pulses per second emitted) are usually much higher with greater distance accuracies realized than for time-of-flight scanners. See Table 3.1 for the technical data of the FARO Focus^{3D} 120.

Each sample tree was scanned from three locations around its periphery at distances ranging from approximately 3-8m away from the tree. To the best extent possible, scan positions were placed at 120° apart from each other to maximize the information gathered for characterizing the geometric shape of the tree. For automatic co-registration, four manually placed targets were positioned near the sample tree with a minimum three targets being visible from each scan position. Targets construction consisted of printed checkerboard signs affixed to wooden staked panel boards (Figure 3.1). Because maximizing information gathered was desired for this study, minimal amounts of understory vegetation deemed obstructive were manually removed.

Scanning was conducted at a speed of 122,000 pulses per second for approximately seven minutes per scan. With transport and setup time between scan positions taking an average of 2-3 minutes, scanning each tree from all three angles took on average 25-30 minutes. Prior determination of target placement typically added an additional 5 minutes, and vegetation removal, if deemed necessary, added anywhere from 5 to 60 minutes for two physically capable crew members.

TLS Point Cloud Registration and Processing

The scan data collected at each scan position was part of its own coordinate system with the scanner location itself as the origin. In order to fuse all three scan positions into one global coordinate system, a process known as registration was necessary. Registration uses common reference objects visible in all scans by assigning the location of those objects to a new general coordinate system to create one registered scan. Registration was done automatically by uploading the scan data

into SCENE v4.8 software (FARO 2014). SCENE software is capable of automatically recognizing the printed checkerboard targets within each scan image for subsequent automatic registration. Quality of registration was reported as tension; the average discrepancy in distance, over the entire global coordinate system, between a given pair of reference objects. Tensions were generally reported as ranging from 1mm to 8mm. An automated procedure was used for noise reduction and filtration of stray points. For each registered scan, the portion of the point cloud that corresponded to the sample tree and its near vicinity was selected visually from the 3D representation of the surrounding forest (Figures 3.2 and 3.3). These selected points were then exported for later use in extracting DBH, HT and HTCB using Matlab 2013b (The MathWorks, http://www.mathworks.com, USA).

Tree Parameter Extraction from Selected Scan Data

Digital Terrain Model

The initial step for extracting the input variables from the point clouds was the creation of a digital terrain model (DTM) for representation of the ground elevations near the sample trees. This process involved first creating an XY-grid of even spacing for each scan, then systematically determining and selecting the point in each grid cell with the lowest elevation, or Z coordinate. The Z coordinate of these selected points were used to represent the elevation of the area their respective grid cells covered. In order to take advantage of the fact that TLS scans yield a much high number of ground-returned points that ALS scans, a 0.3048m × 0.3048m grid size was chosen as

the optimal grid size so that sufficient detail was preserved while the spatial resolution was not greater than the point density on the ground.

Tree Detection

With the ground model complete the next step before obtaining tree parameters was to estimate the center of the sample tree at approximately 1.37m above the ground. This estimated location served as a control point from which all measurement algorithms originated from. As per Mass et al. (2008) the process began by taking a thin 5-10cm thick horizontal slice from the point cloud to use as a subset for estimation (Figure 3.4). This horizontal slice often included many points representing branches and foliage at that height. To expedite the estimation process, only a subset of the points in the slice was used. This subset was created by first graphically determining the XY range of the main bole, and then selecting only the points within that range (Figure 3.5). This subset contains predominantly points returned from the bole, with a minimal number of returns representing other features such as branches, foliage, lichen and moss.

With this subset of points representing a slice of the outside of the bark on the main bole, a nonlinear least squares circle-fitting procedure, similar to that described by Henning and Radtke (2006), was used for estimating the diameter and XY center of the tree. A non-linear least squares optimization function was used for this task. Initial estimates, or starting values, for the diameter and XY center were required as inputs. The two starting values for the XY center that worked well were the means of the XY coordinates of all subset points, provided there were no far outlying points (Maisonobe

2007). Restriction of the subset to the XY range of the main bole additionally addresses any outliers. The starting value for the diameter of the sample tree consisted of using the following equation to solve for a diameter for each of the subset points, and then using the mean of all calculated diameters, produced using the following equation (Henning and Radtke 2006):

$$\hat{d}_i = 2 \times \sqrt{(\hat{x}_c - x_i)^2 + (\hat{y}_c - y_i)^2}$$

where $\hat{d}_i$ is estimated diameter for the i^{th} subset point, the $(\hat{x}_c, \hat{y}_c)$ pair are the means of the (x,y) coordinates for all subset points and the (x_i, y_i) pair are the (x,y) coordinates of the i^{th} subset point. With these three starting values and the following equation as the objective function, the three unknowns were solved for by minimizing the sum of squares for all subset points:

$$F_i = 2 \times \sqrt{(\hat{x}_c - x_i)^2 + (\hat{y}_c - y_i)^2} - \hat{d}_i$$

where F_i is the value of the objective function for the i^{th} subset point and $\hat{x}_c$, $\hat{y}_c$ and $\hat{d}_i$ are the three unknowns. With the spatial location of the center of the tree and its diameter approximated, subsequent measurements stemmed from this information.

Uphill Side of the Tree and Total Height

As is common in forest inventories, when measuring DBH, HT and HTCB for the standing and downed tree measurements, all heights up the bole to the tip of the sample trees were relative to the ground adjacent to the tree with the highest elevation

(Avery and Burkhart 2002, p.144). Thus, it was necessary to identify the uphill-side of the tree and determine the elevation of that side relative to the rest of the point cloud. Using the approximated center and diameter, all DTM cells determined to be spatially adjacent to the base of the sample tree were selected. These cells represented a discrete elevation profile surrounding the base of the tree. The selected DTM cell with the highest elevation value was determined to be the uphill-side of the tree. The corresponding elevation value of that cell, heretofore referred to as the reference z-value, was used as the minimum reference height for extracting DBH, HT and HTCB.

A statistical quality control was implemented in order to ensure the reference z-value was not a far outlier representing anomalies such as nearby rocks or protruding tree roots. Whereby, if the coefficient of variation (CV) of the elevation values of all the selected adjacent DTM cells was above a defined percentage, the adjacent cell with the next highest elevation value was chosen. For this study, the defined CV of 60% was observed to be sufficient in removing the far outliers that occurred. HT was then simply calculated as the difference between the highest point in the point cloud and the reference z-value. Stray points above the tip of the tree were not observed to be a problem due to the prior filtering done in SCENE.

Diameter at Breast Height

While the approximated diameter from the detection slice at 1.37m could serve as an estimate of DBH, the height at which the slice was taken was 1.37m above the minimum elevation of the entire point cloud, rather than the uphill side of the tree. On steeply sloping terrain, differences in relative bole heights could be substantial.

Therefore, an improved DBH was extracted 1.37m above the reference z-value using the previously described procedure of subsetting followed by the non-linear least squares circle-fitting. However, an additional precision constraint was added to maximize the reliability of the DBH measurement. If the root mean square error (RMSE) of the non-linear least squares procedure was above a defined threshold of 5mm, a recursive "noise reduction" method, similar to Henning and Radtke (2006), was invoked. This process involved continually removing the points whose estimated diameters were the maximum absolute distance from the mean of all estimated diameters until the standard deviation of the estimated diameters was below the same defined threshold. It was observed that using 5mm for this threshold was sufficient for minimizing the measurement error, while also removing stray points around, and not belonging to, the main bole.

Height to Crown Base

The majority of methods used to quantify crown-related variables such as HTCB using LiDAR data are based upon return intensity, point frequency and percentile analysis of return height. Return intensity is a measure of the returned energy of an emitted pulse. This value differs depending on a number of variables having to do with environmental conditions, scanner properties, scanner location and, most notably, the surface of reflectance. Using the latter notion, it is possible to exploit differences in return intensities between foliage and woody surfaces for estimating HTCB.

In order to estimate HTCB in this study, two approaches which combine these metrics were examined. The first approach, proposed by Popescu and Zhao (2007) for ALS data, involved polynomial fitting to frequency height profiles of individual tree crowns. Profiles were created by binning point returns into height bins of size 3.048cm for point frequency (Figure 3.6). Fourth-degree polynomials were then fit to these profiles, with return height as the input variable and point frequency as the response variable. The height of the first inflection point of the fitted polynomial, at the lower end of the height profile, was theorized to coincide with the location of HTCB (Figure 3.7).

This second approach consisted of using different percentile heights within a subset of points whose intensity values were below a subjectively determined threshold. By plotting intensity versus height, a subjective determination of an approximate threshold could be determined, below which the intensity values for points returned from foliage would theoretically occur (Figure 3.8). The subset of points below this threshold served as a representation of the live crown profiles.

Using the height of the lowest point in this subset as a measure of HTCB resulted in consistent underestimation, similar to the results observed by Chasmer et al. (2006). This was likely due to: (1) the presence of dead branches interspersed within the lower portion of the live crown, as is common for lodgepole pine; and (2) the definition of HTCB used in this study being the height to the lowest live limb rather than the height to the lower margin of the main live crown. Thus, HTCB was then estimated as the 5^{th}, 10^{th} and 25^{th} percentile height of this subset for the 20-40yr,

40-80yr and >80yr age classes of sample trees selected, respectively. Selection of this threshold was based upon: (1) empirical observation; and (2) the knowledge that younger lodgepole pine trees typically have lower HTCB values and fewer dead branches. Due to this method yielding the lowest average measurement error, the measurements resulting from this approach were ultimately selected for use in the subsequent error propagation analysis.

Error Propagation

For DBH, HT and HTCB, the differences between the TLS measurements and the downed-tree measurements were calculated for all 25 trees. The same was done for HT and HTCB for the standing tree measurements for all 25 trees. Measurement error variability was quantified following the same methodology described in Chapter 2. Monte Carlo simulations, also mirroring those described in Chapter 2, were used to quantify the propagated error associated with both instrument measurements using the CRM equations.

Results and Discussion

Measurement Errors

Table 3.2 shows the measurement error summary statistics for input variable measurements using the TLS and the standing tree measurements (STM). The circle-fitting procedure for measuring DBH worked quite well overall, with 6 of the 25 trees showing exact agreement with the downed tree measurements, and 9 being within 3.048cm. These results are comparably better than previous studies assessing the quality of TLS-derived diameter measurements. Somonse et al. (2003) used a Hough-

transformation to obtain DBH for 23 trees, reporting minimum, maximum, mean and standard deviation of measurement error values as -5.8cm, 5.6cm, 1.7cm and 2.8cm, respectively. Hopkinson et al. (2004) reported an average difference of 10cm for plot-level comparison of DBH between TLS and manual measurement techniques. Thies et al. (2004) used a stem reconstruction method involving the fitting of a series of cylinders up the main stem of two scanned deciduous trees of different species. DBH was calculated as the diameter of the corresponding cylinder at breast height. Deviations in TLS-derived DBH measurements from standing tree measurements were -1.3cm (3.3in) and 0.6cm (1.5in) for European beech and wild cherry, respectively. Henning and Radtke (2006) reported errors of less than 1cm (0.3in) using a similar circle-fitting procedure as the one described here when comparing TLS diameters to known values from felled trees. In a separate study attempting to model 3D plot-level forest structure, Henning and Radtke (2006) reported an average DBH difference of 4.8cm when comparing TLS measurements to standing tree measurements. It is reasonable to believe the quality of these TLS-derived DBH results compared to other studies is largely attributable our multi-scan approach, which has been shown to reduce the variability TLS-derived DBH measurements (Pueschel et al. 2013).

It was observed using a RMSE threshold below 5mm generally resulted in underestimations of DBH. This was due to points on the outside of the fissures of the bark being the points removed first during this point removal process. Because the true values of DBH were measured on the outside of these fissures, stricter thresholds were not used. Hence, if this procedure is to be used for older trees of a species with deeply fissured bark characteristics, this process may require allowing for higher RMSE

thresholds. Average RMSE observed for the fitting of all 25 DBHs was 3.99mm. This process holds promise for obtaining upper stem diameters outside bark for purposes of taper determination, form factor calculation and possible merchantable height identification as well.

HT measurement error results for TLS showed lower average bias than the STM HT measurements at -0.1m and -1.0m for TLS and STM, respectively. Encouragingly, the standard deviation of these measurement errors for HT was also lower for TLS, at 0.3m and 0.7m for TLS and STM, respectively. Hopkinson et al. (2004) reported an average difference of 1.5m for plot-level HT comparisons between TLS and manual measurement techniques. Their reported difference in standard deviations of HT measurements was lower at 0.2m. Chasmer et al (2006) reported an average underestimation of HT of 1.2m for 15 trees within a closed-canopy stand of red pine (*Pinus resinosa*) scanned from five different locations. The comparative improvement upon these studies suggests this method of identifying a reference z-value from which to subtract from the maximum z-value is superior to other methods. However, with stand density and tree size being limiting factors in the accuracy of TLS-derived-HT measurements, the quality of the results we present here for HT could also likely be a result of several of the sample trees being from stands with lower stand densities, and lodgepole pine being a relatively shorter tree species. The capability of the FARO Focus^{3D} 120 to scan at the point density chosen for this study also likely furthered this improvement.

In contrast to HT, HTCB results for the TLS exhibited a larger mean and standard deviation of the measurement errors compared to the STM. However, this variable has typically been a point of imprecision for TLS extraction procedures. As mentioned previously, Chasmer et al. (2006) reported average differences in HTCB measurements from "actual" values of 6.4m. The author's HTCB measurement method was the identifying of the "lowest apparent base-of-live-crown" point. Thies et al. (2004) reported HTCB values of -0.12m and -0.11m for the two aforementioned sample trees. With the sample trees being relatively large, forked and deciduous, HTCB was measured as the height to the first fork. Jung et al. (2011) compared HTCB measurements from coincident ALS and TLS data, where the TLS measurements were considered to be the actual values. ALS HTCB values were obtained using k-means clustering technique which groups the point cloud into a user-defined number of classifications based upon differences in the spatial distribution of points within the point cloud. The authors chose three classifications to represent ground cover, understory vegetation and canopy cover. ALS HTCB was determined from the lowest point in the canopy cover classification. Because differences in the point density distribution were deemed too small with the TLS data, k-means clustering was not used, replaced by manual identification of the lowest crown return via a monitor display. The difference in mean HTCB values was reported as 0.2m.

With a wider array of techniques already developed for obtaining HTCB from ALS data than TLS data, the interest in assessing the efficacy of the Popescu et al. (2007) polynomial fitting method for use in TLS applications was deemed worthwhile. Measurement error minimum, maximum, mean and standard deviation for HTCB

using the polynomial fitting method with intensity as the response variable were -5.8m, 8.2m, 4.2m and 4.0m, respectively. Average measurement error for this method ended up being 3.7m greater than the subsetted percentile-height method with the difference in standard deviations of measurement error being 2.3m.

Applying the TLS inventory parameter extraction techniques used here to broad-scale inventory data with several million trees would be time efficient; however, future improvements would further bolster the applicability of TLS to larger operations. First, rather than the manual graphical method for tree detection employed here, more sophisticated automatic tree detection procedures that omit non-bole points from branches and foliage, would be necessary. Secondly, for the subsetted percentile approach for HTCB, the tree size to percentile relationship may need to be more generalized by diameter classes, or calibrated to the specific operation.

Model Predictions and Uncertainty

Once the predicted CRM component ratios were produced, they were multiplied by the predicted total tree biomass obtained using the SUR equation. When measurement error was not integrated into the model errors, differences in results from those discussed in Chapter 2 for the CRM equations were negligible (Table 3.3). When measurement error was integrated into the CRM equations, mean predictions for all components and total tree-level AGB were very comparable between instruments (Table 3.4). The TLS RMSE values for the CRM ratios were lower for all components compared to the STM RMSE values (Table 3.5). However, the RMSE of the tree-level predictions was 35.9% larger for the TLS, primarily due to the SUR

equation having a 147% larger RMSE. This can be attributed to the assumption that the STM measurement of DBH, the only input variable for the SUR equation, was measured without error, hence the STM simulation procedure did not involve the contamination of DBH values. Had measurement error in DBH been assessed, it is not unfair to reason that the uncertainty value for the STM SUR equation would be greater than the 70.59kg value reported here. Also worthy of noting, the magnitude of the difference between STM and TLS may be less dramatic with the use of a separate total tree equation, that wasn't fit within a separate system of equations. Nevertheless, the tree-level uncertainty in predicted component AGB associated with using the TLS for extracting input variables for the CRM equations is depicted here as likely being greater that a spencer tape used by trained individuals.

Per Unit Area Estimates and Uncertainty

Similar to the tree-level results, when only sampling error is considered for per unit area estimation, the standard error of the means between the two sets of equations show a similar trend observed in Chapter 2 (Table 2.6). With model errors incorporated into the simulations for per unit area estimation, the uncertainty increases nearly fourfold due to the issues discussed in Chapter 2 concerning serial correlation between the total tree and component predictions (Table 3.7). This dramatic increase is further illustrated in Table 3.8, where the RSE values for all component and total increased two to threefold. Encouragingly, though, was the notable difference in per unit area precision between instruments when measurement error was integrated, with the total uncertainty associated with using STM being 6% higher than with using the

TLS (Table 3.9). Difference in total RSE values for STM versus TLS was 2.3%, with the STM RSE values being higher at 54.5% and the TLS RSE values being 52.1%. Similar to Chapter 2 CRM results, the relative proportions of SE due to measurement, model and sampling error using SRM were 11%, 66% and 23%, respectively. The increase in the proportion due to model error from 55% to 66% from the previous chapter's values was attributed to the smaller data set used here. The relative proportions of SE due to measurement, model and sampling error using the TLS were 5%, 70% and 25%, respectively. These results suggest using the TLS can result in a lower propagated error, primarily due to a smaller contribution to the total uncertainty from measurement error.

Conclusion

With broad-scale inventories, such as FIA and others, likely to face an increased demand for defensible AGB uncertainty estimates, accounting for and addressing all primary sources of error becomes paramount. Taking the Monte Carlo approach shown here, measurement and model error have been successfully integrated and accounted for with relative ease. Furthering the point made about inferential limits in Chapter 2, with only 25 instead of 32 subjectively selected trees for use in comparison, the bias in uncertainty estimation is likely more pronounced in this study than the previous. However, not only were the general contributions for all three sources of error illustrated, the addressal of measurement error was made by showing that the use of the TLS indeed can improve precision of per unit area estimation of lodgepole pine AGB using the CRM equations presented here.

The prior recommendation of accounting for the correlation structure of the combined CRM equations bears worth re-mentioning, as this would likely provide a better depiction of the gains in precision to be had by using the TLS in conjunction with the CRM equations. Future research into this matter could also be best directed at similarly assessing the propagated error from using the TLS with other AGB models, as well as models for other parameters of interests, both point-in-time and growth-related. Nevertheless, these results imply the TLS data analysis techniques shown here hold value in reducing uncertainty attributed to measurement error, which has been shown to contribute a potentially serious amount to the total per unit area uncertainty for the CRM estimates

References

Avery, T. E., and Burkhart, H. E. (2002). Forest measurements (No. Ed. 5). McGraw-Hill Book Company.

Bienert, A., Scheller, S., Keane, E., Mullooly, G., and Mohan, F. 2006. Application of terrestrial laser scanners for the determination of forest inventory parameters. International Archives of Photogrammetry, Remote Sensing and Spatial Information Sciences. 36(5).

Chasmer, L., Hopkinson, C., and Treitz, P. 2006. Investigating laser pulse penetration through a conifer canopy by integrating airborne and terrestrial lidar. Can. J. of Rem. Sens. 32(2):116-125.

FARO. 2014. Techsheet of Laser Scanner FARO Focus^{3D} 120. http://www.faro.com

Henning, J. G., and Radtke, P. J. 2006. Detailed stem measurements of standing trees from ground-based scanning lidar. For. Sci. 52(1): 67-80.

Henning, J. G., and Radtke, P. J. (2006). Ground-based laser imaging for assessing three dimensional forest canopy structures. Photo. Eng. and Rem. Sens. 72(12): 1349.

Hopkinson, C., Chasmer, L., Young-Pow, C., and Treitz, P. 2004. Assessing forest metrics with a ground-based scanning lidar. Can. J. of For. Res. 34(3): 573-583.

Jung, S. E., Kwak, D. A., Park, T., Lee, W. K., and Yoo, S. 2011. Estimating crown variables of individual trees using airborne and terrestrial laser scanners. Rem. Sens. 3(11): 2346- 2363.

Maas, H. G., Bienert, A., Scheller, S., and Keane, E. 2008. Automatic forest inventory parameter determination from terrestrial laser scanner data. Int.J. of Rem. Sens. 29(5): 1579-1593.

Maisonobe, L. 2007. Finding the circle that best fits a set of points. October 25th.

MATLAB version 2013b. Natick, Massachusetts: The MathWorks Inc., 2013

Popescu, S. C., and Zhao, K. 2008. A voxel-based lidar method for estimating crown base height for deciduous and pine trees. Remote Sensing of Environment. 112(3):767-781.

Pueschel, P., Newnham, G., Rock, G., Udelhoven, T., Werner, W., and Hill, J. 2013. The influence of scan mode and circle fitting on tree stem detection, stem diameter and volume extraction from terrestrial laser scans. ISPRS J. of Photo. and Rem. Sen. (77):44-56.

Simonse, M., Aschoff, T., Spiecker, H., and Thies, M. 2003Automatic determination of forest inventory parameters using terrestrial laser scanning. Proceedings of the ScandLaser Scientific Workshop on Airborne laser scanning of forests. 2003: 252-258.

Thies M., Pfeifer, N., Winterhalder, D., and Gorte, B. G. 2004. Three-dimensional reconstruction of stems for assessment of taper, sweep and lean based on laser scanning of standing trees. Scand. J.of For.Res. 19(6): 571-581.

Weiß, J. 2009. Application and statistical analysis of terrestrial laser scanning and forest growth simulations to determine selected characteristics of Douglas-Fir stands. Folia For Pol. Ser A(51): 123-137.

Yu, X., Liang, X., Hyyppä, J., Kankare, V., Vastaranta, M., and Holopainen, M. 2013. Stem biomass estimation based on stem reconstruction from terrestrial laser scanning point clouds. Rem. Sens. Lett. 4(4): 344-353.

Table 3.1: TLS technical data

Specification	Focus^{3D} 120
Range Finder	Phase shift
Field of view (horizontal x vertical)	360° x 305°
Measurement range	0.6m – 120m
Distance accuracy	± 2mm at 25m
Sampling Rate	Up to 976k/sec
Beam radius at discharge	3.0mm
Beam divergence	0.19mrad (0.011°)
Weight	5.0kg

Table 3.2: Summary statistics of the measurements errors for STM and TLS

Standing Tree Measurements (STM)					
	n	**Min.**	**Mean**	**Max.**	**SD**
HT (m)	25	-2.56	-0.98	0.12	0.67
HTCB (m)	25	-1.04	-0.06	1.37	0.52
Terrestrial LiDAR (TLS)					
	n	**Min.**	**Mean**	**Max.**	**SD**
DBH (cm)	25	-1.27	-0.25	1.52	0.51
HT (m)	25	-0.79	-0.06	0.55	0.27
HTCB (m)	25	-3.29	0.49	3.90	1.68

Table 3.3: Model predictions and RMSE values for CRM ratios and CRM tree-level estimates without measurement error. Tree-levels units are in kilograms of dry biomass.

Model Means-Without Measurement Error			Model RMSEs-Without Measurement Error		
Total Tree (SUR)	287.11		**Total Tree (SUR)**	70.59	
Component	**CRM Ratios**	**CRM Tree-Level**	**Component**	**CRM Ratios**	**CRM Tree-Level**
Bole	0.672	193.07	**Bole**	0.067	51.24
Bark	0.055	15.66	**Bark**	0.034	10.62
Branch	0.195	56.04	**Branch**	0.055	21.02
Foliage	0.082	23.40	**Foliage**	0.022	8.63
Total	**1.004**	**288.17**	**Total**	**0.179**	**91.50**

Table 3.4: Model predictions for CRM ratios and CRM tree-level estimates with measurement error, for STM and TLS. Tree-levels units are in kilograms of dry biomass.

Model Means-With Measurement Error				
Total Tree (SUR)-STM	287.11			
Total Tree (SUR)-TLS	296.57			
	STM	**TLS**	**STM**	**TLS**
Component	**CRM Ratios**	**CRM Ratios**	**CRM Tree-Level**	**CRM Tree-Level**
Bole	0.599	0.620	172.03	177.97
Bark	0.061	0.061	17.45	17.47
Branch	0.209	0.208	60.11	59.80
Foliage	0.091	0.091	26.19	26.21
Total	0.961	0.980	275.78	281.45

Table 3.5: Model RMSE values for CRM ratios and CRM tree-level estimates with measurement error, for STM and TLS. Tree-levels units are in kilograms of dry biomass.

Model RMSEs-With Measurement Error				
Total Tree (SUR)-STM	70.59			
Total Tree (SUR)-TLS	174.70			
	STM	**TLS**	**STM**	**TLS**
Component	**CRM Ratios**	**CRM Ratios**	**CRM Tree-Level**	**CRM Tree-Level**
Bole	0.297	0.067	95.30	123.09
Bark	0.047	0.034	14.04	15.16
Branch	0.074	0.055	25.81	43.16
Foliage	0.037	0.022	12.46	19.19
Total	0.455	0.179	147.61	200.61

Table 3.6: Per hectare estimates and SE values for CRM equations, without accounting for measurement or model error. Units are in kilograms of dry biomass per hectare.

Sampling Error Only		
Component	**Mean**	**SE**
Bole	23,270.38	4,945.90
Bark	1,842.11	357.83
Branch	6,414.97	1,234.54
Foliage	2,544.31	463.86
Total	**31,527.46**	**6,538.27**

Table 3.7: Per hectare estimates and SE values for CRM equations accounting for model error. Units are in dry kilograms of biomass per hectare.

Sampling Error (With Model Error)		
Component	**Mean**	**SE**
Bole	37,062.80	17,659.36
Bark	4,947.56	3,317.42
Branch	9,275.29	4,043.61
Foliage	3,425.94	1,234.22
Total	**51,285.65**	**25,020.39**

Table 3.8: Per hectare estimates and SE values for CRM equations accounting for model error. Units are in dry kilograms of biomass per hectare.

Sampling Error (With Model and Measurement Error)					
	Mean			**SE**	
Component	**STM**	**TLS**	**Component**	**STM**	**TLS**
Bole	37,819.12	37,442.94	**Bole**	19,201.47	18,583.77
Bark	3,984.19	3,740.49	**Bark**	4,502.45	3,429.02
Branch	9,475.49	9,475.52	**Branch**	4,266.80	4,363.27
Foliage	3,512.56	3,547.24	**Foliage**	1,316.67	1,355.31
Total	**51,278.80**	**50,658.95**	**Total**	27,970.72	26,376.05

Table 3.9: RSE values for CRM equations accounting for model and measurement error.

Sampling Error (RSEs)				
	Sampling Only	**Model Errors**	**Model and Measurement Errors**	
Component			**STM**	**TLS**
Bole	21.3%	47.6%	50.8%	49.6%
Bark	19.4%	67.1%	113.0%	91.7%
Branch	19.2%	43.6%	45.0%	46.0%
Foliage	18.2%	36.0%	37.5%	38.2%
Total	**20.7%**	**48.8%**	**54.5%**	**52.1%**

Figure 3.1: Planar view of scan points depicting typical field scanning setup with four checkerboard targets setup around the sample tree, located middle right.

Figure 3.2: Filtered overhead 3D view of registered point cloud. Black circles denote scan locations around the sample tree, located right center.

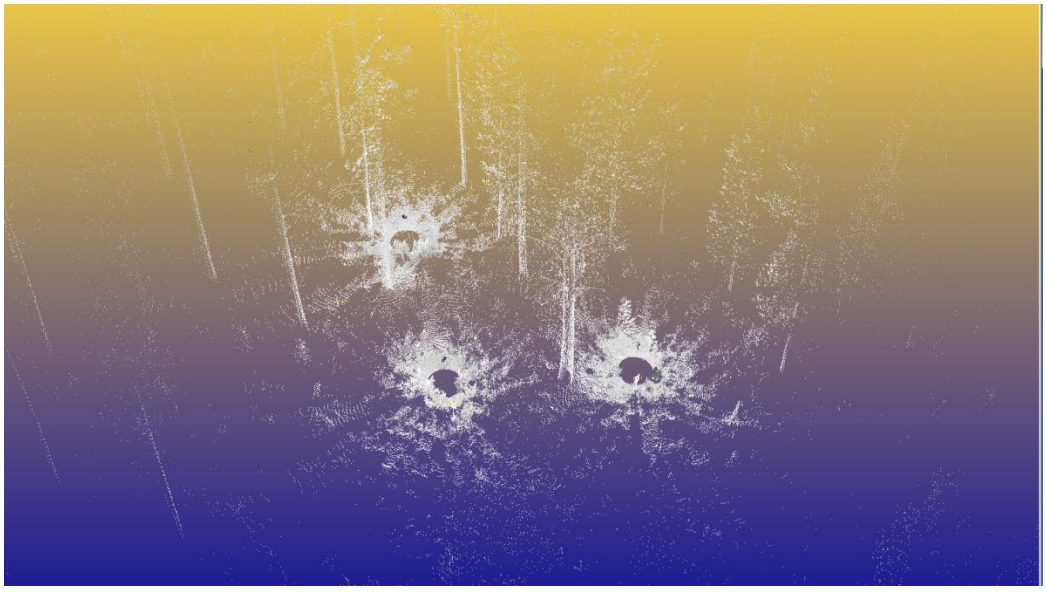

Figure 3.3: Clipped sample tree from surrounding forest depicted in Figure 2.2.

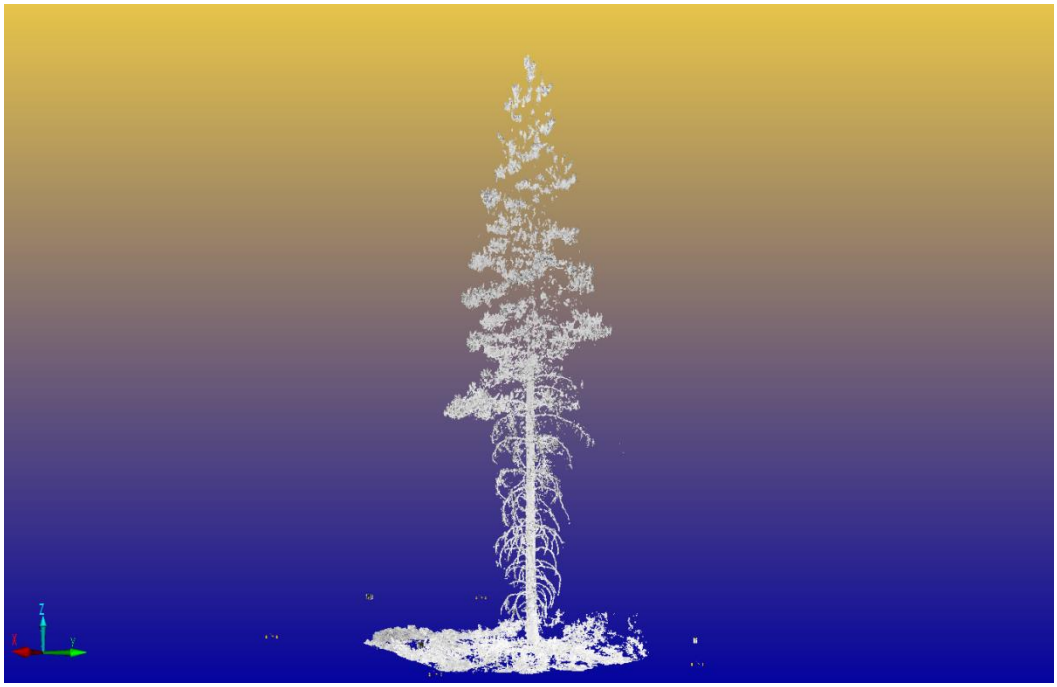

Figure 3.4: Birds eye view of detection slice taken at 1.37m above the lowest point in the point cloud. Unrestricted subset included branches and foliage located within the height range of the slice.

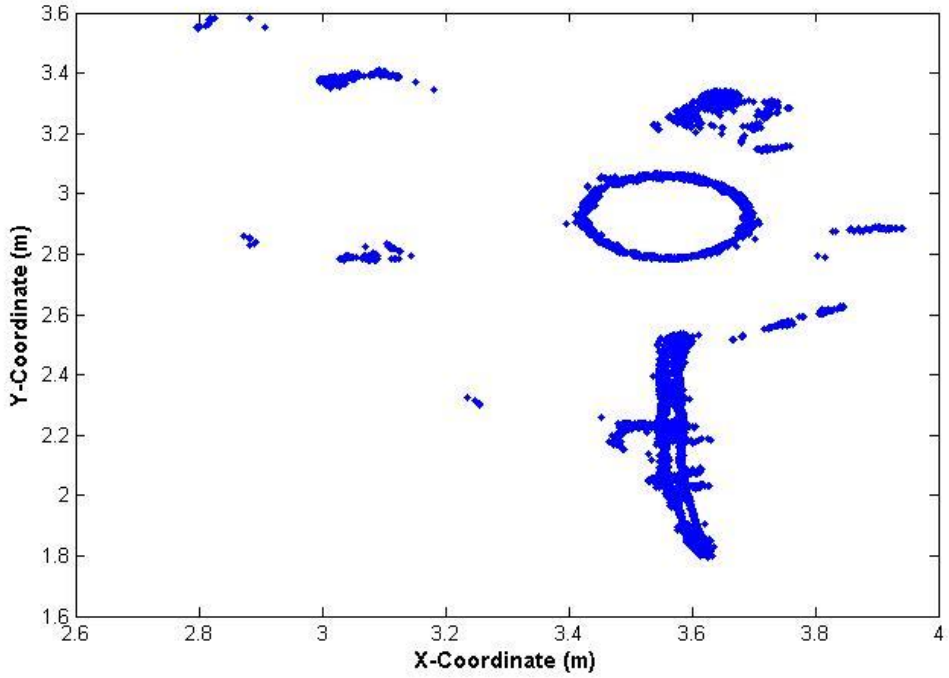

Figure 3.5: Birds eye view of detection slice taken at 1.37m above the lowest point in the point cloud. Unrestricted subset included branches and foliage located within the height range of the slice.

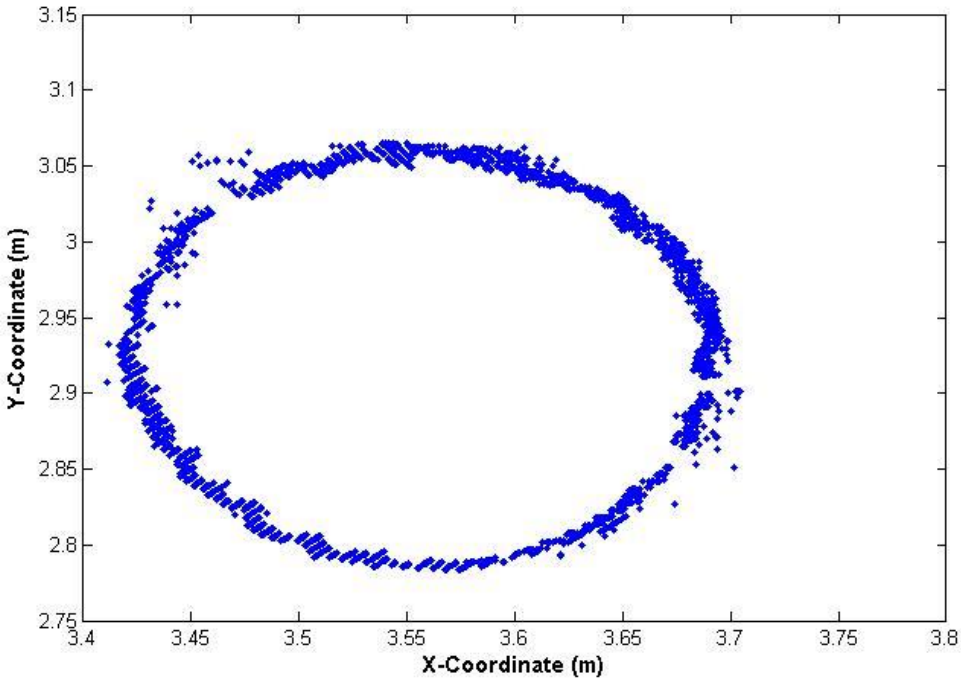

Figure 3.6: Graph of point frequency versus elevation, depicting the 0.1m height bins. Actual total tree height is 16.95m.

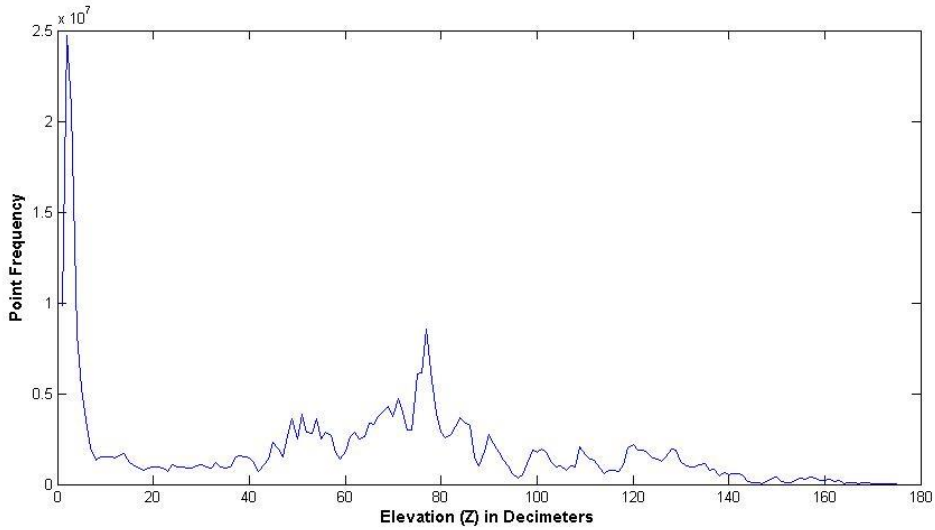

Figure 3.7: Fourth-order Polynomial Fit to the Frequency Height Profile. The first inflection point from the ground was theorized to correspond to the location of HTCB.

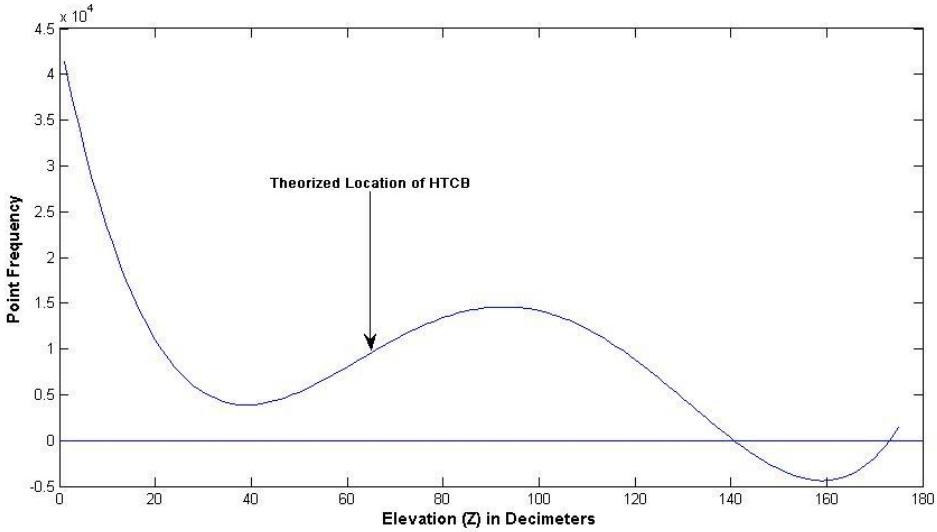

Figure 3.8: Graph of intensity values versus elevation for 0.1m height bins. Subjectively determined subset threshold is shown in red.

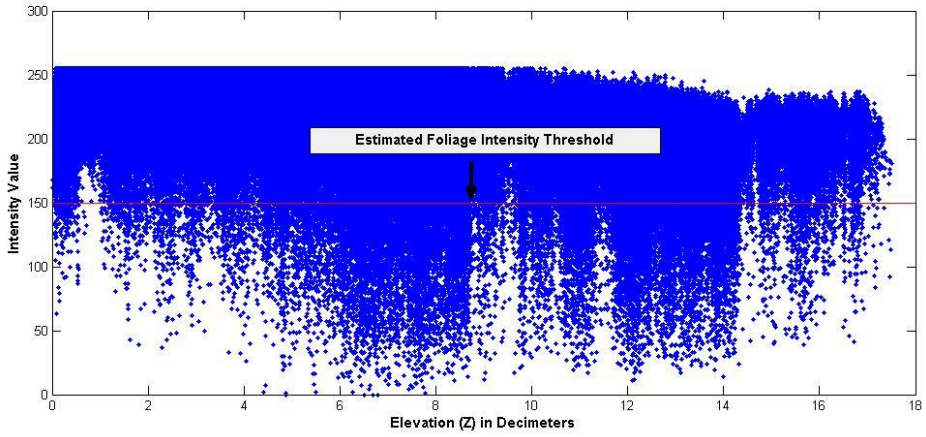

Chapter 4: General Conclusion

This aims of this study included the assessment and comparison of uncertainty for two sets of equations for lodgepole pine AGB for use in the Pacific Northwest, with an additional aim to compare the capabilities of two sets of instruments in reducing total uncertainty due to measurement error. The two sets of equations compared were the CRM and current regional models for lodgepole pine AGB used by FIA. The instrument comparison made was between a FARO Focus^{3D} 120 and the combination of a Trupulse Laser Rangefinder 360R and a Spencer combination tape. Monte Carlo simulations were used for propagating measurement, model and sampling error and to compare total uncertainty between models, and between instruments. Input variables for the equations were DBH, HT and HTCB; these were extracted from the TLS point clouds through the creation of automated algorithms. Additionally, the uncertainty due to measurement error was found to be lower when using the TLS versus the standing tree measurements.

The scope of inference for this study is limited by a number of different factors. The relatively small portion of the range of lodgepole pine that was covered for creation of the CRM equations limits the inference for the entirety of the region these equations are intended to represent. Additionally, with a relatively small sample size of subjectively selected trees, the uncertainty results observed for both sets of equations and instruments are indeed approximations, likely having some amount of bias. Furthermore, only a majority, rather than all, of the trees used for the creation of the CRM equations were scanned by the TLS, also rendering as approximations the

inferences about total uncertainty due to measurement error. Despite these inferential limits, these findings can be as a basis for deciding which equations set is desirable for use. The relative contributions of each source of error also provide depictions of which error source is of most concern for each equation set, and for each set of instruments. This study is also the first to the author's knowledge to illustrate that the TLS holds legitimate value in reducing broad-scale uncertainty due to measurement error.

The second chapter of this study specifically compared the relative contributions of measurement, model and sampling error between the newly-created CRM equations and the current regional equations for lodgepole pine. The CRM equations were found to be less precise than the current regional equations with the integration of all three sources of uncertainty. This is due to the hierarchical nature of the CRM approach, where two estimates that are highly correlated, with their own respective sources of uncertainty, are multiplied together to produce total component AGB. These findings can be used as a validation for the continued use of the current regional lodgepole pine equations in the Pacific Northwest region.

The third chapter of this study specifically compared the relative contribution of measurement error to total uncertainty estimates of AGB using both terrestrial LiDAR and traditional inventory instruments. This assessment was done using the CRM equations in an attempt to illustrate the ameliorative effect of using a high precision TLS to reduce the already-inflated total uncertainty associated with these equations. Results showed the total uncertainty associated with using the TLS being lower than the standing tree measurements by a difference of 2.3% in RSE. While this

difference could be deemed small for these point-in-time estimates, with monitoring programs performing multiple re-measurements over time, where there is an even greater need for standardized and precise measurements, the significance of these results suggest the TLS could further reduce uncertainty for trend estimation purposes. Hence, this information may provide an impetus for its future assimilation into various forest inventory and monitoring programs, such as FIA, as a valuable tool for increasing precision of the status and trend of AGB estimates.

In order to ascertain the exact contribution of model uncertainty using the CRM equations presented here, future research efforts will need to take into account the correlation structure between the total tree biomass equation and the component ratio equations. Use of Bayesian Markov Chain Monte Carlo simulations would be the logical next step in accounting for this correlation structure. Future studies are also well positioned to easily take the methods presented here and apply them to other species-specific equations for AGB. Investigations into using the same multi-scan approach for plot-level analysis would add credence to the work done here, as that is likely the more applicable inventory scenario forest managers would be utilizing the TLS, rather than for single trees, as was done in this study. Extraction of additional tree-level input variables, such as upper stem diameters, merchantable top height and crown width would provide additional information about how the performance of the TLS in extracting these variables propagates up to per unit estimates of AGB. All of these future research efforts stand to increase the defensibility of reported precision estimates for AGB derived using individual-tree equations, while also helping determine under which scanning scenarios, and for which input variables, does the use

of the TLS translate into quantifiable gains in precision for broad-scale estimates of AGB.

BIBLIOGRAPHY

Avery, T. E., and Burkhart, H. E. (2002). Forest measurements (No. Ed. 5). McGraw-Hill Book Company.

Baskerville, G.L. 1972. Use of logarithmic regression in the estimation of plant biomass. Can. J. of For. Res. 2(1):49-53

Behre, C.E. 1926. Comparison of diameter tape and caliper measurements in second-growth spruce. J. Forestry., 24(2):178-182

Berger. A., Gschwantner, R.E., McRoberts, R.E., and Schadauer, K. 2014. Effects of measurement errors on individual tree stem volume estimates for the Austrian National Forest Inventory. For. Sci. 60(1):14-24

Bell, J.F., and Gourley, R. 1980. Assessing the accuracy of a sectional pole, Haga altimeter, and alti-level for determining total height of young coniferous stands. South. J. of App. For. 4(3):136-138

Bienert, A., Scheller, S., Keane, E., Mullooly, G., and Mohan, F. 2006. Application of terrestrial laser scanners for the determination of forest inventory parameters. International Archives of Photogrammetry, Remote Sensing and Spatial Information Sciences. 36(5).

Brackett, M. 1977. Note on TARIF tree-volume computation. DNR Rep. 24. Olympia, WA: Washington Department of Natural Resources. 132p

Breidenbach, J., Antón-Fernández, C., Petersson H., Astrup, P., and McRoberts, R.E. 2014. Quantifying the model-related variability of biomass stock and change estimates in the Norwegian National Forest Inventory. For. Sci. 60(1):25-33

Canavan, S.J., and Hann, D.W. 2004. The two-stage method for measurement error characterization. For. Sci. 50(6):743-756

Chasmer, L., Hopkinson, C., and Treitz, P. 2006. Investigating laser pulse penetration through a conifer canopy by integrating airborne and terrestrial lidar. Can. J. of Rem. Sens. 32(2):116-125.

Chave, J., Condit, R., Aguilar, S., Hernandez, A., Lao, S., and Perez, R. 2004. Error propagation and scaling in tropical forest biomass estimates. Philos. Trans. R. Soc. Lond. B 359(1443):409:420

Chojnacky, David C. 2012. FIA's volume-to-biomass conversion method (CRM) generally underestimates biomass in comparison to published equations. Moving from Status to Trends: Forest Inventory and Analysis (FIA) Symposium 2012, pp. 396-402. GTR-NRS- P-105. US Department of Agriculture, Forest Service, Northern Research Station.

Cunia, T. 1965. Some theory on reliability of volume estimates in a forest inventory sample. For. Sci., 11(1):115-128.

FARO. 2014. Techsheet of Laser Scanner FARO Focus^{3D} 120. http://www.faro.com

Forest Products Laboratory. 2010. Wood handbook—Wood as an engineering material. Gen. Tech. Rep. FPL-GTR-190. Madison, WI: U.S. Department of Agriculture, Forest Service, Forest Products Laboratory. 508 p

Freese, F., 1961.Relation of plot size to variability: an approximation. J. Forestry. 59:679

Gertner, G.Z. 1990. The sensitivity of measurement error in stand volume estimation. Can. J. of For. Res. 20(6):800-804

Gray, A. 2003. Monitoring stand structure in mature coastal Douglas-fir forests: effect of plot size. For. Ecol. Manage., 175(1):1-16.

Heath, L.S., M.H. Hansen, J.E. Smith, W.B. Smith, and P.D. Miles. 2008. Investigation into calculating tree biomass and carbon in the FIADB using a biomass expansion factor approach. In: McWilliams, W.; Moisen, G.; Czaplewski, R., comps. 208 Forest Inventory and Analysis (FIA) symposium. Proc. RMRS-P-56 CD. Fort Collins, CO: U.S. Department of Agriculture, Forest Service, Rocky Mountain Research Station. [CD–ROM].

Henning, J. G., and Radtke, P. J. 2006. Detailed stem measurements of standing trees from ground-based scanning lidar. For. Sci. 52(1):67-80.

Henning, J. G., and Radtke, P. J. (2006). Ground-based laser imaging for assessing three dimensional forest canopy structures. Photo. Eng. and Rem. Sens. 72(12):1349.

Hopkinson, C., Chasmer, L., Young-Pow, C., and Treitz, P. 2004. Assessing forest metrics with a ground-based scanning lidar. Can. J. of For. Res. 34(3): 573-583.

Hosmer, D.W., Lemeshow, S. 1989. Applied Logistic Regression. New York: John Wiley & Sons, Inc. 307p

Jenkins, J.C., Chojnacky, D.C., Heath, L.S., and Birdsey, R.A. 2003. National-scale biomass estimators for United States tree species. For. Sci. 49(1):12.-35

Johnson, F.A., Hixon, H.J., 1952. The most efficient size and shape of plot to use for cruising in old-growth Douglas-fir timber. J. For. 50(1):17-20

Jung, S. E., Kwak, D. A., Park, T., Lee, W. K., and Yoo, S. 2011. Estimating crown variables of individual trees using airborne and terrestrial laser scanners. Rem. Sens. 3(11): 2346-2363.

Kalliovirta, J., Laasasenaho, J., and Kangas, A. 2004. Evaluation of the laser-relaskop. For. Ecol. Manage. 204:171-194

Kutner, M.H., Nachtsheim, C.J., Neter, J. 2004. Applied Linear Regression Models. McGraw-Hill/Irwin.

Lu, Dengsheng. 2006. The potential and challenge of remote sensing-based biomass estimation, Int. J. of Rem. Sens. 27(7):1297-1328.

Maas, H. G., Bienert, A., Scheller, S., and Keane, E. 2008. Automatic forest inventory parameter determination from terrestrial laser scanner data. Int.J. of Rem. Sens. 29(5): 1579-1593.

Maisonobe, L. 2007. Finding the circle that best fits a set of points. October 25th.

MATLAB version 2013b. Natick, Massachusetts: The MathWorks Inc., 2013

McRoberts, R.E., Hahn, J.T., Hefty G.J., and Van Cleve, J.R. 1994. Variation in forest inventory field measurements. Can. J. For. Res. 24:1766-1770.

McRoberts, R.E., and Westfall, J.A. 2014. Effects of uncertainty in model predictions of individual tree volume on large area volume estimates. For. Sci. 60(1):34-42

Mowrer, H.T., and Frayer, W.E. 1986. Variance propagation in growth and yield projections. Can. J. of For. Res. 16(6):1196-1200

Plamondon, J. A. 1999. Log-length measurement errors with six single-grip harvester heads. Technical Note Forest Engineering Research Institute of Canada - FERIC, No. TN-297. 6p.

Popescu, S. C., and Zhao, K. 2008. A voxel-based lidar method for estimating crown base height for deciduous and pine trees. Remote Sensing of Environment. 112(3):767-781.

Pueschel, P., Newnham, G., Rock, G., Udelhoven, T., Werner, W., and Hill, J. 2013. The influence of scan mode and circle fitting on tree stem detection, stem diameter and volume extraction from terrestrial laser scans. ISPRS J. of Photo. and Rem. Sen. (77) :44-56.

R Core Team (2012). R: A language and environment for statistical computing. R Foundation for Statistical Computing, Vienna, Austria. ISBN 3-900051-07-0, URL http://www.Rproject.org/

SAS Institute Inc. Output for this paper was generated using SAS software, Version 9.4 of the SAS System for Windows. Copyright © 2013 SAS Institute Inc. SAS and all other SAS Institute Inc. product or service names are registered trademarks or trademarks of SAS Institute Inc., Cary, NC, USA.

Simonse, M., Aschoff, T., Spiecker, H., and Thies, M. 2003Automatic determination of forest inventory parameters using terrestrial laserscanning. Proceedings of the ScandLaser Scientific Workshop on Airborne laser scanning of forests. 2003: 252-258.

Skovsgaard, J.P., Johannsen, V.K., and Vanclay, J.K. 1998. Accuracy and precision of two laser dendrometers. Forestry 71:131-139

Ståhl, G., Heikkinen, J., Petersson, H., Repola, J., and Holm, S. 2014. Sample-based estimation of greenhouse gas emissions from forests-a new approach to account for both sampling and model errors. For. Sc. 60(1):3-13.

Standish, J.T., Manning, G.H., and Demaerschalk, J.P. 1985. Development of biomass equations for British Columbia tree species. Information Report BC-X-264. Canadian Forest Service, Pacific Resource Center. 47p

Suty, N., Nyström, K., and Ståhl, G. (2013). Assessment of bias due to random measurement errors in stem volume growth estimation by the Swedish National Forest Inventory. Scand. J.of For.Res.28(2):174-183.

Thies M., Pfeifer, N., Winterhalder, D., and Gorte, B. G. 2004. Three-dimensional reconstruction of stems for assessment of taper, sweep and lean based on laser scanning of standing trees. Scand. J.of For.Res. 19(6):571-581.

Vanclay, J.K., Skovsgaard, J.P. 1997. Evaluating forest growth models. Ecol. Model. 98(1):1-12

Weiß, J. 2009. Application and statistical analysis of terrestrial laser scanning and forest growth simulations to determine selected characteristics of Douglas-Fir stands. Folia For Pol. Ser A(51):123-137.

Weiskittel, A. R., Hann, D. W., Kershaw Jr, J. A., and Vanclay, J. K. 2011. Forest growth and yield modeling. John Wiley & Sons.

Wesfall, J.A., and Patterson, P.L. 2007. Measurement variability error for estimates of volume change. Can J. of For. 37(11):2201-2210

Williams, M.S., Bechtold, W.A., and LaBau, V.J. 1994. Five instruments for measuring tree height: An evaluation. South. J. App. For. 18(2):76-82.

Woodall, C.W., Heath, L.S., Domke, G.M., and Nichols, M.C. 2011. Methods and equations for estimating aboveground volume, biomass, and carbon for trees in the U.S. forest inventory, 2010. Gen. Tech. Rep. NRS-88. Newton Square, PA: U.S. Department of Agriculture, Forest Service, Northern Research Station. 30p

Yu, X., Liang, X., Hyyppä, J., Kankare, V., Vastaranta, M., and Holopainen, M. 2013. Stem biomass estimation based on stem reconstruction from terrestrial laser scanning point clouds. Rem. Sens. Lett. 4(4):344-353.

Zhou, X. P., and Hemstrom, M. A. 2009. Estimating aboveground tree biomass on forest land in the Pacific Northwest: a comparison of approaches. Res. Pap. PNW-RP-584. Portland, OR: U.S. Department of Agriculture, Forest Service, Pacific Northwest Research Station. 18p

Zhou, X. P., and Hemstrom, M. A. 2010. Timber volume and aboveground live tree biomass estimations for landscape analyses in the Pacific Northwest. Gen. Tech. Rep. PNW-GTR- 819. Portland, OR: U.S. Department of Agriculture, Forest Service, Pacific Northwest Research Station. 31 p

APPENDIX

LIST OF ACRONYMS USED IN TEXT

Acronym	Definition
AGB	Aboveground biomass
ALS	Airborne laser scanner
CRM	Component ratio method
CRM-FIA	Component ratio method used by FIA
CV	Coefficient of variation
DBH	Diameter at breast height
DNF	Deschutes National Forest
DOB	Diameter outside bark
DTM	Digital terrain model
FIA	Forest Inventory and Analysis
HT	Total tree height
HTCB	Height to the base of live crown
LiDAR	Light detection and ranging
NFI	National Forest Inventory
RMSE	Root mean square error
RRMSE	Relative root mean square error
RSE	Relative standard error
SE	Standard error
STM	Standing tree measurements
SUR	Seemingly unrelated regression
TLS	Terrestrial laser scanner
TTWOF	Total tree aboveground biomass without foliage
WNF	Willamette National Forest